Hindawi Publishing Corporation
ISRN Corrosion
Volume 2013, Article ID 703929, 22 pages
http://dx.doi.org/10.1155/2013/703929

Research Article

Corrosion Inhibition of Cu-Ni (90/10) Alloy in Seawater and Sulphide-Polluted Seawater Environments by 1,2,3-Benzotriazole

Venkata Appa Rao Boyapati and Chaitanya Kumar Kanukula

Department of Chemistry, National Institute of Technology Warangal (NIT Warangal), Warangal, Andhra Pradesh 506 004, India

Correspondence should be addressed to Venkata Appa Rao Boyapati; boyapativapparao@rediffmail.com

Received 31 October 2012; Accepted 27 November 2012

Academic Editors: W. Fuerbeth and S. J. Lee

The inhibiting effect of 1,2,3-benzotriazole (BTAH) against the corrosion of Cu-Ni (90/10) alloy in seawater and seawater polluted with inorganic sulphide was studied by electrochemical impedance studies (EISs), potentiodynamic polarization studies, and cyclic voltammetric (CV) and weight-loss studies. Surface examination studies were carried out by X-ray photo electron spectroscopy (XPS) and scanning electron microscopy (SEM)/energy dispersive X-ray analysis (EDX). EIS studies have been carried out in seawater and 10 ppm of inorganic sulphide containing seawater in the absence and presence of BTAH at different concentrations, different immersion periods, and at different temperatures. Appropriate equivalent circuit model was used to calculate the impedance parameters. The potentiodynamic polarization studies inferred that BTAH functions as a mixed inhibitor. The impedance, polarization, and weight-loss studies showed that the inhibition efficiency of BTAH is in the range between 99.97 and 99.30% under different conditions. Cyclic voltammeric studies show the stability of the protective BTAH film even at anodic potentials of +550 mV versus Ag/AgCl. All these studies infer that BTAH functions as an excellent inhibitor for Cu-Ni (90/10) alloy in seawater and sulphide-polluted seawater. XPS and SEM-EDX studies confirm the presence of protective BTAH film on the alloy surface.

1. Introduction

Copper-nickel alloys are extensively used in marine applications because of their good electrical and thermal conductivities, corrosion resistance, and ease of fabrication of the equipment [1]. The 90/10 copper-nickel alloy is a material of selection for condensers and heat exchangers, where seawater is used as a coolant and in desalination plants [2, 3]. This alloy is resistant to stress corrosion cracking by ammonia and sulphide ions [4] and has good resistance to biofouling due to the release of copper ions [5, 6]. This alloy is also resistant to pitting and crevice corrosion in quiet seawater [7]. The corrosion resistance of this alloy is related to the performance of the passive film, which is mainly composed of Cu_2O [8–11], though other copper (II) based compounds such as atacamite and cupric oxide are also present in the film [6] after long exposure. The cupric species generally overlies the cuprous species. However, in the sulphide containing seawater, the corrosion rate of Cu-Ni (90/10) alloy is increased as the sulphide ions interfere with the film formation and produce a nonprotective black layer containing cuprous oxide and sulphide ions. The pollution of seawater with sulphide ions at the coastal areas can occur due to industrial waste water discharges into sea and also due to biological and bacteriological processes taking place in seawater. Thus, corrosion of Cu-Ni (90/10) alloy in seawater polluted with sulphide ions is a serious problem, which has drawn the attention of the researchers in this field. Sayed et al. [12] studied the corrosion behaviour of Cu-Ni (90/10) alloy in 3.5% sodium chloride solution in the absence and presence of different concentrations of sulphide ions in the range from 100 to 1000 ppm by potentiodynamic polarization studies and surface analysis by scanning electron microscopy and X-ray diffraction technique. They found that the corrosion

rate of the alloy increased in the presence of sulphide ions and at a very high concentration of S^{2-}, the alloy suffered from pitting corrosion. Hack [13] reported that the required concentration of S^{2-} to increase the corrosion susceptibility of Cu-Ni (90/10) alloy may be as low as 0.01 ppm. De Sanchez and Schiffrin [14] studied the disruptive effect of sulphide ions on the protective film formed on Cu-Ni (90/10) alloy in seawater polluted with sulphides.

Organic inhibitors have been reported in the literature to protect Cu-Ni alloys from corrosion in different environments [15, 16]. The heterocyclic organic compounds, namely, azoles, were reported to show marked inhibition efficiency on corrosion of Cu-Ni alloys [17, 18]. Omar et al. [19] studied the corrosion inhibition of Cu-Ni (90/10) alloy in 0.5% hydrochloric acid and 0.5% sulfuric acid solutions by using Schiff bases as corrosion inhibitors. Badawy et al. [20] studied the corrosion inhibition of Cu-5Ni and Cu-65Ni alloys in 0.6 mol dm^{-3} chloride solution using amino acids as inhibitors. Benmessaoud et al. [15] studied the inhibiting effect of 2-mercaptobenzimidazole against the corrosion of 70Cu-30Ni alloy in aerated 3% sodium chloride solution polluted with ammonia (pH = 9.25) by potentiodynamic polarization studies and electrochemical impedance studies. 1,2,3-benzotriazole is a well-known corrosion inhibitor for copper. Babic et al. [21] studied the inhibiting effect of benzotriazole against corrosion of Cu-Ni (90/10) alloy in 1 M sodium acetate solution by cyclic voltammetry, photopotential measurements, and impedance spectroscopy. Allam et al. [22] studied the effect of benzotriazole on the corrosion of Cu-Ni (90/10) alloy in 3.4% sodium chloride solution containing 2 ppm of sulphide ions by weight-loss measurements and X-ray diffraction technique. Maciel and Agostinho [23] employed the potentiodynamic polarization studies on the Cu-Ni (90/10) alloy rotating disc electrode in deaerated 0.5 mol L^{-1} sulfuric acid solution containing Fe(III) ions as oxidant and benzotriazole as inhibitor and showed that benzotriazole at a concentration $>1.0 \times 10^{-3}$ mol L^{-1} afforded an excellent inhibition. Nevertheless, no studies have been reported in the literature on the corrosion behaviour of Cu-Ni (90/10) alloy in seawater and sulphide-polluted seawater in the presence of 1,2,3-benzotriazole at different immersion periods and at different temperatures. Studies using cyclic voltammetry have not been reported on benzotriazole as inhibitor for Cu-Ni (90/10) alloy in seawater and sulphide-polluted seawater. A comprehensive study, employing electrochemical impedance, potentiodynamic polarization, cyclic voltammetry, weight-loss studies, XPS, and SEM-EDX on corrosion inhibition of Cu-Ni (90/10) alloy in seawater and sulphide containing seawater environments by 1,2,3-benzotriazole (BTAH), has been attempted in the present work.

2. Experimental

2.1. Materials. The composition of Cu-Ni (90/10) alloy used in the present study is given in Table 1. The composition of synthetic seawater is given in Table 2 [24]. All the chemicals used in the preparation of synthetic seawater were of AnalaR grade. A stock solution of 1000 ppm of inorganic sulphide containing seawater was prepared by dissolving 2.44 g of AnalaR sodium sulphide in synthetic seawater and making the solution up to the mark in 1000 mL standard measuring flask. From this stock solution, 10 ppm of sulphide containing seawater was prepared. 1,2,3-benzotriazole obtained from Sigma-Aldrich was used as such. The cupronickel alloy specimens were taken from the same Cu-Ni (90/10) alloy sheet. For electrochemical studies, specimens with the dimensions of 4.0 × 1.0 × 0.2 cm were used by exposing 1 cm^2 surface area, while the remaining area was insulated with epoxy resin. For weight-loss studies also, 4.0 × 1.0 × 0.2 cm specimens were used. For XPS and SEM-EDX studies, 1.0 × 1.0 × 0.2 cm and 0.5 × 0.5 × 0.2 cm specimens were used, respectively. All these specimens were polished with 1/0, 2/0, 3/0, and 4/0 grade emery papers consecutively. Later these specimens were polished to mirror finish with alumina and water slurry on the micro polishing cloth, which is fixed on the rotating disc polishing machine. Then, these specimens were washed with triple distilled water, degreased with acetone and dried by blowing N_2 gas for 20 minutes. These specimens were tested in different corrosive environments.

2.2. Electrochemical Studies. Electrochemical impedance studies were carried out in a three-electrode cell assembly (in accordance with ASTM specifications) using an electrochemical work station, model IM6e Zahner-Elektrik, Germany. The Cu-Ni (90/10) alloy of the surface area of 1 cm^2 was used as the working electrode in the absence and presence of BTAH in seawater and sulphide-polluted seawater environments. A platinum electrode was used as the counter electrode and the reference electrode was Ag/AgCl/1.0 M KCl electrode. The impedance studies were carried out at the open circuit potential (OCP) in the frequency range from 60 kHz to 10 mHz under the excitation of sinusoidal wave of ±5 mV amplitude.

The potentiodynamic polarization studies and cyclic voltammetric studies were carried out by using the same three-electrode cell assembly and the electrochemical work station as described under impedance studies. The potentiodynamic polarization studies were conducted in the potential range of −0.7 V to +0.7 V versus Ag/AgCl with a scan rate of 1 mVs^{-1}. The cyclic voltammetric studies were carried out in the potential range of −1.0 V to +1.0 V versus Ag/AgCl with a scan rate of 10 mVs^{-1}. All the electrochemical studies were conducted at different immersion periods in the range from 1 to 48 h. The impedance studies were carried out at three different temperatures, namely, 30, 40, and 60°C.

2.3. Gravimetric Measurements. In all the gravimetric experiments, the polished Cu-Ni (90/10) alloy specimens were weighed and immersed in duplicate, in 500 mL seawater and 10 ppm of inorganic sulphide containing seawater in the absence and presence of BTAH at two different concentrations, for a period of 30 days. Then these specimens were reweighed after dipping for 2 to 3 min in hydrochloric acid (1 + 1) or sulfuric acid (1 + 10) at room temperature. Later, these specimens were scrubbed with a bristle brush under

Table 1: Composition of the Cu-Ni (90/10) alloy.

Element	Cu	Ni	Fe	Mn	Pb	Al	Others in trace amounts
Composition (%)	88.512	9.882	1.086	0.412	0.046	0.038	0.024

Table 2: Composition of the synthetic seawater.

Compound name	NaCl	KCl	$MgCl_2{\cdot}6H_2O$	$CaCl_2$	$MgSO_4{\cdot}7H_2O$	$NaHCO_3$	KBr	H_3BO_3	$SrCl_2{\cdot}6H_2O$	NaF
$g\,L^{-1}$	27.24	1.40	10.11	2.28	13.92	0.39	0.20	0.026	0.04	0.006

running water, degreased with acetone, and dried. During the studies, only those results were taken into consideration, in which the difference in the weight loss of the two specimens immersed in the same solution did not exceed 0.1 mg. Accuracy in weighing up to 0.01 mg is recommended by ASTM G31 guidelines [25]. The immersion period of 30 days was fixed in view of the considerable magnitude of the corrosion rate obtained in the absence of any inhibitor after this immersion period. Under these conditions of accuracy, the relative standard error in corrosion rate determinations is of the order of 2% or less [26]. Corrosion rates (CRs) of alloy specimens in the absence and presence of BTAH are expressed in mmpy. Inhibition efficiencies of the inhibitor were calculated by using the formula:

$$\text{IE}\ (\%) = \frac{[(\text{CR})_0 - (\text{CR})_I]}{(\text{CR})_0} \times 100, \tag{1}$$

where $(\text{CR})_0$ and $(\text{CR})_I$ are the corrosion rates in the absence and presence of BTAH, respectively.

2.4. Surface Analytical Techniques. The surface analysis of Cu-Ni (90/10) alloy in the absence and presence of BTAH was carried out using the X-ray photoelectron spectrometer, ESCA Kratos model AXIS-165, with Mg Kα radiation (1253.6 eV) and energy resolution of 0.1 eV. Computer deconvolution was applied to detect the elemental peaks of copper, oxygen, carbon, nitrogen, and sulfur present on the surface of the alloy. SEM-EDX studies were carried out using JEOL JSM-6390LV/LGS Scanning Electron Microscope, USA, and JEOL Model JED-2300, Energy Dispersive X-ray Analyzer, USA.

3. Results and Discussion

3.1. Electrochemical Impedance Studies. Figures 1(a) and 1(b) show the Nyquist and Bode plots of Cu-Ni (90/10) alloy in synthetic seawater in the absence of BTAH at different immersion periods in the range from 1 to 48 h. The corresponding impedance parameters are given in Table 3. The Nyquist plots exhibit diffusion impedance at all the immersion periods. The diameter of semicircular region increases with immersion time. This means that there is an increase in the charge transfer resistance (R_{ct}) with the increase in immersion time. The total impedance Bode plot also indicates that the impedance increases with the immersion time. The phase angle Bode plots reveal that the phase maximum is the same at 1- and 3-hour immersion periods and it shifts to a lower frequency at higher immersion periods. There is only one maximum in all these plots and the angle corresponding to phase maximum is found to increase from 51° at 1-hour immersion time to 56° at 48-hour immersion time. All the above results infer that with the increase in immersion time, the film is becoming more and more protective. In these figures the $|Z|$ versus f curves exhibit three distinctive segments. In the high frequency extreme region, the value of $|Z|$ tends to become very small and the corresponding phase angle also falls off very rapidly with increasing frequency. This region is typical of a resistive behaviour and corresponds to solution resistance. In the medium frequency region, a linear relationship exists between $|Z|$ and f and there is a broad maximum in the phase angle versus frequency plot. This region corresponds to the charge transfer at the metal/electrical double layer. In the low frequency segment, the resistive behaviour of the electrode increases and the value of $|Z|$ should remain constant with a further decrease in frequency. But such behaviour is not found. $|Z|$ still increases, with a decrease in frequency. This corresponds to the diffusion impedance because of the diffusion of oxygen and chloride from the bulk of the solution to the interface at the instant of the immersion of the electrode in synthetic seawater and also of $CuCl_2^-$ species from the interface into the bulk of the solution at higher immersion periods, besides diffusion of oxygen and chloride from solution to the interface [27, 28]. In order to account for the above results, the metal/solution interface is modeled as per the equivalent circuit shown in Figure 2(a) [24] and the best fit is obtained for the experimental results with this model. In this model constant phase element (CPE) is substituted for the double layer capacitance to give a more accurate fit [29]. The CPE is a special element whose admittance value is a function of the angular frequency (ω) and whose phase is independent of frequency. Its admittance and impedance components are given in the following equations, respectively:

$$Y_{\text{CPE}} = Y_0(j\omega)^n, \tag{2}$$

$$Y_{\text{CPE}} = \frac{1}{\left[Y_0(j\omega)^n\right]}. \tag{3}$$

Y_0 is the magnitude of the CPE, j is the imaginary number ($j = (-1)^{1/2}$), and ω ($= 2\pi f$) is the angular frequency [30]. The factor "n" is the adjustable parameter that usually lies between 0 and 1 [31]. The CPE describes an ideal capacitor when n is equal to 1 [29, 31]. Both the charge transfer resistance of the double layer (R_{ct}) and the film resistance (R_{film}) are found to increase with immersion period. The "n"

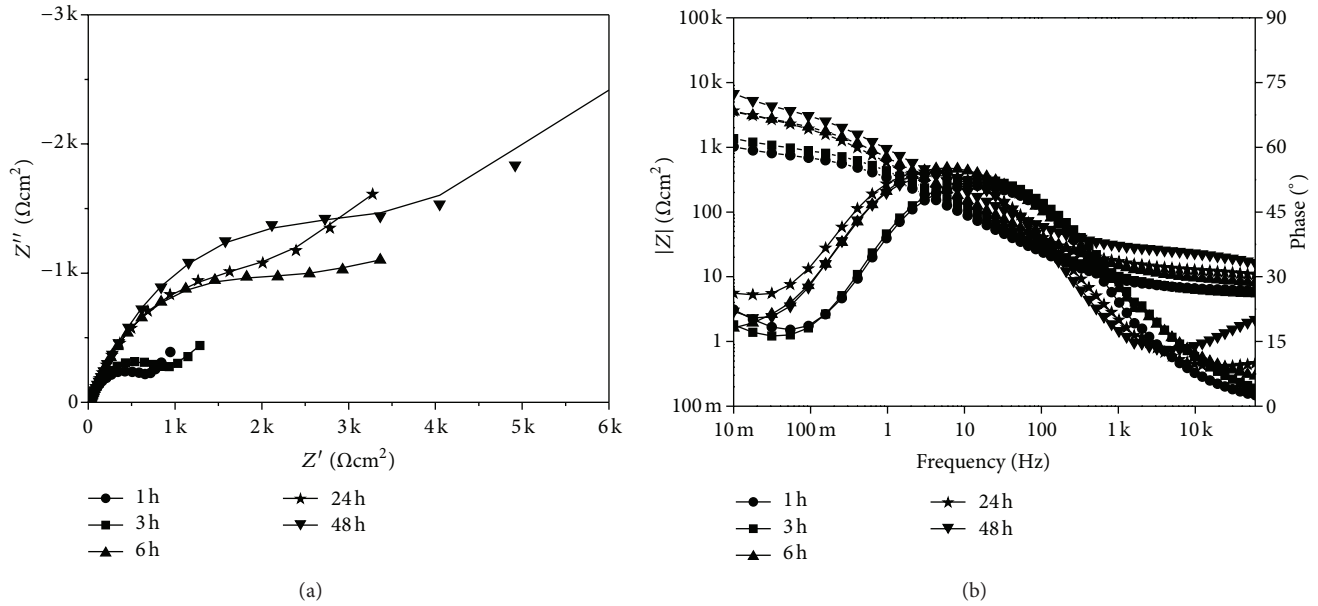

Figure 1: (a) Nyquist and (b) Bode plots of Cu-Ni (90/10) alloy in synthetic seawater at different immersion periods. –●–: 1 h, –■–: 3 h, –▲–: 6 h, –★–: 24 h, and –▼–: 48 h. (Temperature: 30°C).

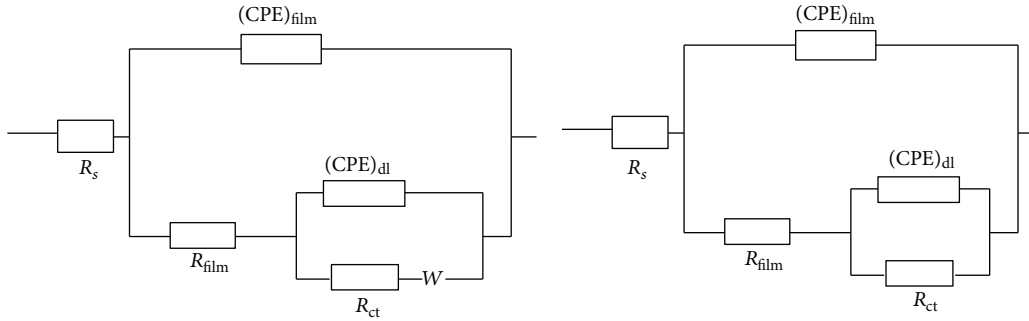

R_{ct}: charge transfer resistance
CPE: constant phase element
W: Warburg impedance
R_s: solution resistance
R_{film} : film resistance
$(CPE)_{film}$: constant phase element of lm
$(CPE)_{dl}$: constant phase element of double layer

(a)

R_{ct}: charge transfer resistance
CPE: constant phase element
W: Warburg impedance
R_s: solution resistance
R_{film} : film resistance
$(CPE)_{film}$: constant phase element of lm
$(CPE)_{dl}$: constant phase element of double layer

(b)

Figure 2: Equivalent circuits used to calculate the impedance parameters.

values corresponding to both the CPE of double layer and of the film are found to increase slightly with the increase in immersion period.

Figures 3(a) and 3(b) show the Nyquist and Bode plots, respectively, of the Cu-Ni (90/10) alloy in seawater containing 1,2,3-benzotriazole inhibitor at various concentrations, namely, 0.82, 1.67, 2.50, and 3.33 mM at a constant immersion period of 48 h. The Nyquist plots are not perfect semicircles. With increasing concentration, the diameter of the semicircle is found to increase. Though there is absence of Warburg-like behaviour, the plots show a combination of a semicircle and a linear (horizontal) pattern. These results in the low frequency region indicate the resistive behaviour of the alloy. The Bode plots are quite interesting. The phase angle Bode plots show that there is a shift of frequency corresponding to phase maximum from about 5 Hz in the absence of BTAH to a much higher frequency of the order of kHz in the presence of 0.82 mM BTAH. The angle corresponding to phase maximum is also increased from 56° to about 75°. A close examination of these plots reveals that there is a possibility of two time constants. It is interesting to note that with a further increase in the concentration of the inhibitor to 3.33 mM, there is a shift in the phase maximum to a lower frequency side and phase angle is increased to about

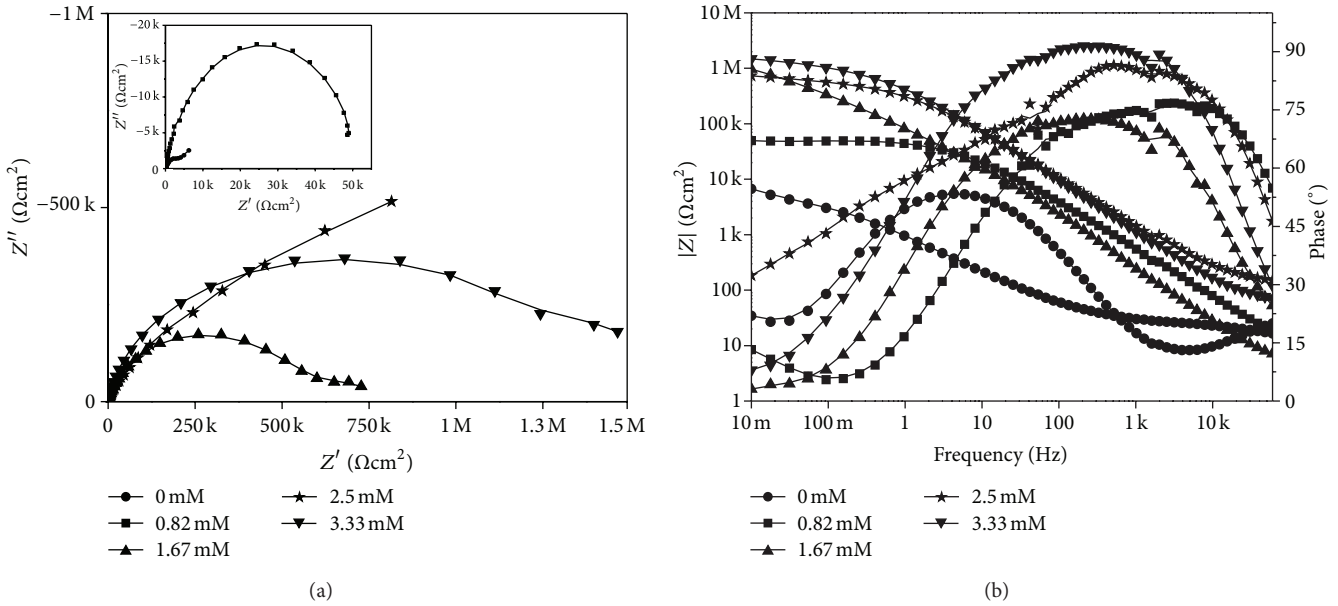

Figure 3: (a) Nyquist and (b) Bode plots of Cu-Ni (90/10) alloy in synthetic seawater in the presence of different concentrations of BTAH at 48-hour immersion period. –●–: 0 mM, –■–: 0.82 mM, –▲–: 1.67 mM, –★–: 2.50 mM, and –▼–: 3.33 mM. (Temperature: 30°C).

Table 3: Impedance parameters of Cu-Ni (90/10) alloy in seawater at different immersion periods. (Temperature: 30°C).

Immersion period (h)	R_{ct} ($k\Omega\,cm^2$)	$(CPE)_{dl}$ ($\mu F\,cm^{-2}$)	n_1	R_f ($k\Omega\,cm^2$)	$(CPE)_{film}$ ($\mu F\,cm^{-2}$)	n_2
1	0.722	28.41	0.64	0.002	36.44	0.60
3	1.004	14.50	0.65	0.005	34.81	0.64
6	3.168	13.30	0.66	0.007	27.34	0.64
24	4.174	12.32	0.67	0.008	15.47	0.65
48	4.720	12.20	0.67	0.010	15.12	0.66

80°. The total impedance is increased to a very great extent in the presence of the inhibitor and with the increase in the concentration of the inhibitor. There is more broadening of the phase maximum with the increase in the concentration of the inhibitor. This result reveals that the protective nature of the inhibitor film is increased with the increase in the concentration of the inhibitor. The electrochemical system may be modeled as consisting of metal/protective surface film/electrical double layer/electrolyte solution. Therefore, for all the systems, in the presence of BTAH, the equivalent circuit shown in Figure 2(b) is used. The experimental data fitted with this equivalent circuit better than with other equivalent circuits reported in the literature [16, 20, 24]. The corresponding impedance parameters are given in Table 4. It is interesting to note that both R_{ct} and R_{film} are increased with the increase in the concentration of the inhibitor. An increase in R_{ct} from 4.72 to 1046 $k\Omega\,cm^2$ and an increase in R_{film} from 0.01 to 557.8 $k\Omega\,cm^2$ are obtained by the addition of 3.33 mM of BTAH to seawater. Inhibition efficiencies are calculated from the R_{ct} values in the absence and presence of BTAH using

$$\text{IE}\ (\%) = \left(R_{ct}^1 - \frac{R_{ct}}{R_{ct}^1}\right) \times 100. \quad (4)$$

In (4), R_{ct}^1 and R_{ct} are the charge transfer resistances in the presence and absence of BTAH, respectively. An IE% of 99.55 is obtained at 3.33 mM concentration of BTAH. Both the $(CPE)_{dl}$ and $(CPE)_{film}$ values are reduced to extremely small values of 0.034 and 0.060 $\mu F\,cm^{-2}$, respectively, in the presence of BTAH and the corresponding "n" values are increased to 0.94 and 0.78, respectively. These results reveal that the concentration of BTAH molecules in the protective film is increased and the Cu_2O formation is much less. BTAH molecules replaced almost all the water molecules and the ions in the electrical double layer.

As a protective film with a high charge transfer resistance is formed when the concentration of BTAH is 3.33 mM, it was of interest to investigate the effect of immersion time in the range from 1 to 48 h, on the impedance spectra. The corresponding Nyquist and Bode plots are shown in Figures 4(a) and 4(b), respectively. The impedance parameters are given in Table 5. The Nyquist plots show the absence of Warburg impedance at all immersion periods and the increase in the diameter of the semicircular part of the plots (in the intermediate frequencies) and also the increase in the linear (horizontal) part of the plots in the lower frequency region with increase in the immersion period. The Bode plots reveal

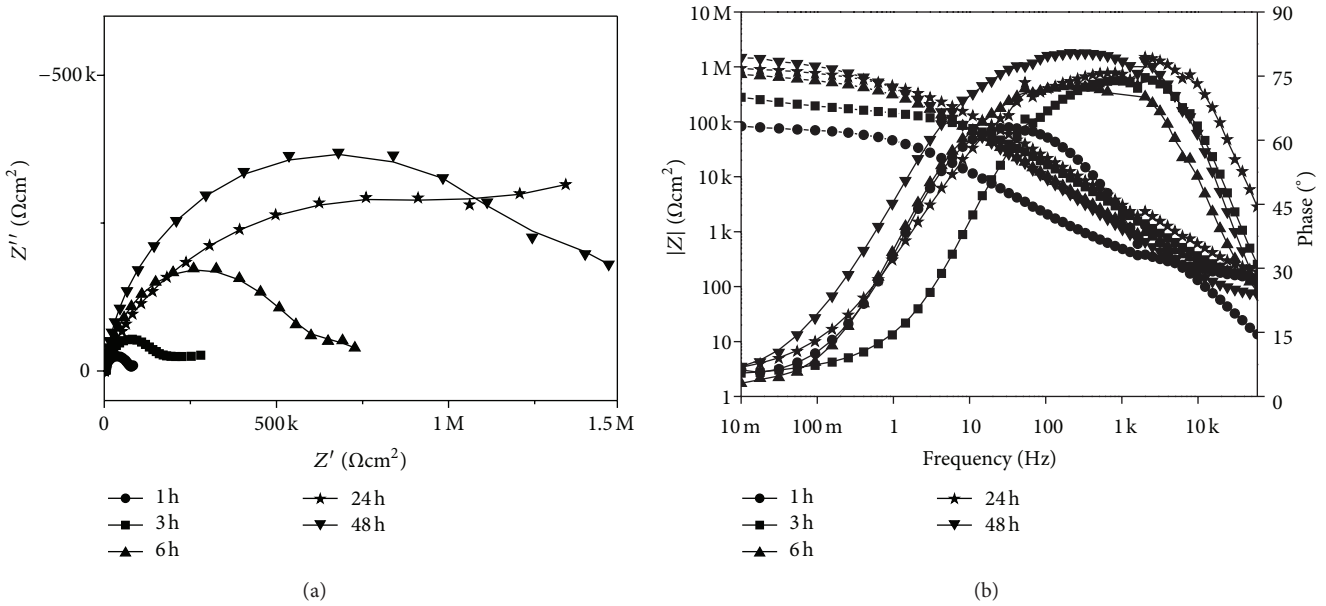

Figure 4: (a) Nyquist and (b) Bode plots of Cu-Ni (90/10) alloy in synthetic seawater in the presence of 3.33 mM BTAH at different immersion periods. –●–: 1 h, –■–: 3 h, –▲–: 6 h, –★–: 24 h, and –▼–: 48 h. (Temperature: 30°C).

Table 4: Impedance parameters of Cu-Ni (90/10) alloy in seawater in the presence of different concentrations of BTAH at 48-hour immersion period. (Temperature: 30°C).

Concentration of BTAH (mM)	R_{ct} (kΩ cm^2)	$(CPE)_{dl}$ (μF cm^{-2})	n_1	R_{film} (kΩ cm^2)	$(CPE)_{film}$ (μF cm^{-2})	n_2	IE (%)
0	4.72	12.20	0.67	0.01	15.12	0.66	—
0.82	44.8	0.096	0.73	5.34	0.290	0.68	89.48
1.67	362.5	0.058	0.84	80.3	0.137	0.72	98.70
2.50	620.3	0.045	0.91	250.6	0.072	0.73	99.24
3.33	1046.0	0.034	0.94	557.8	0.060	0.78	99.55

some interesting features. After 1-hour immersion time, the phase angle Bode plot reveals two phase maxima, one in the high frequency region and one in the mid frequency region. With increase in immersion period, the broadening of the phase maximum and increase in phase angle maximum are quite significant. After 48-hour immersion period, the total impedance Bode plot is linear, almost throughout the frequency region. With increase in immersion time, the slopes of the $|Z|$ versus f plots are found to increase in the lower frequency region while there is almost a merger of these plots somewhere in the middle frequency region after the immersion period ≥3 h.

After the formation of the protective film on the Cu-Ni (90/10) alloy by immersing it in seawater containing 3.33 mM BTAH for 48 h, the effect of the increase of temperature on the impedance behaviour of this prefilmed alloy was studied in seawater containing 3.33 mM BTAH for an immersion period of 48 h at two different temperatures, namely, 40 and 60°C. The nature of Nyquist and Bode plots are similar to those plots at 30°C (plots not shown). However, the total impedance and phase angle maximum values in the Bode plots are reduced with the increase in temperature. Nevertheless, in the absence of BTAH also, the total impedance and phase angle maximum values are reduced with the increase in temperature. The impedance parameters at different temperatures for bare Cu-Ni (90/10) alloy and prefilmed Cu-Ni (90/10) alloy after an immersion period of 48 h in seawater containing 3.33 mM BTAH are given in Table 6. Both R_{ct} and R_{film} of the prefilmed alloy are found to decrease with the increase in temperature. Nevertheless, these values are still far higher in comparison to the corresponding values of the bare alloy. Hence, inhibition efficiencies >99% are obtained even at 40 and 60°C. The increase in $(CPE)_{dl}$ values is not as much as the increase in the $(CPE)_{film}$ values. Both the n_1 and n_2 values are decreased to some extent with the increase in temperature. All these results are indicative of the deviation of double layer and also of the film from more capacitative to less capacitative behaviour.

Figures 5(a) and 5(b) show the Nyquist and Bode plots of Cu-Ni (90/10) alloy in seawater environment containing 10 ppm of inorganic sulphide ions in the absence of BTAH at different immersion periods. The corresponding impedance parameters are given in Table 7. The Nyquist plots show that the real and imaginary parts of the complex impedance decrease to a great extent in comparison to the behaviour of the alloy in the absence of sulphide ions at all

Table 5: Impedance parameters of Cu-Ni (90/10) alloy in seawater in the presence of 3.33 mM BTAH at different immersion periods. (Temperature: 30°C).

Immersion period (h)	R_{ct} ($k\Omega\,cm^2$)	$(CPE)_{dl}$ ($\mu F\,cm^{-2}$)	n_1	R_{film} ($k\Omega\,cm^2$)	$(CPE)_{film}$ ($\mu F\,cm^{-2}$)	n_2	IE (%)
1	66.26	1.732	0.68	14.55	2.546	0.68	98.91
3	142.8	0.064	0.72	117.0	1.321	0.70	99.30
6	379.9	0.055	0.74	227.3	0.141	0.77	99.17
24	882.4	0.022	0.86	762.0	0.077	0.78	99.53
48	1046.0	0.034	0.94	557.8	0.060	0.78	99.55

Table 6: Impedance parameters of Cu-Ni (90/10) alloy in seawater and prefilmed alloy in the presence of 3.33 mM BTAH in seawater at different temperatures. (Immersion period: 48 h).

Specimen	Environment	Temperature	R_{ct} ($k\Omega\,cm^2$)	$(CPE)_{dl}$ ($\mu F\,cm^{-2}$)	n_1	R_{film} ($k\Omega\,cm^2$)	$(CPE)_{film}$ ($\mu F\,cm^{-2}$)	n_2	IE (%)
Bare alloy	Seawater	40	2.972	8.38	0.71	0.004	72.52	0.57	—
Prefilmed alloy	Seawater + 3.33 mM BTAH	40	1231.0	0.310	0.86	237.5	0.493	0.80	99.76
Bare alloy	Seawater	60	0.315	50.42	0.58	0.002	210.0	0.55	—
Prefilmed alloy	Seawater + 3.33 mM BTAH	60	542.0	0.520	0.82	473.0	0.748	0.78	99.94

Table 7: Impedance parameters of Cu-Ni (90/10) alloy in seawater containing 10 ppm of inorganic sulphide at different immersion periods. (Temperature: 30°C).

Immersion period (h)	R_{ct} ($k\Omega\,cm^2$)	$(CPE)_{dl}$ ($\mu F\,cm^{-2}$)	n_1	R_{film} ($k\Omega\,cm^2$)	$(CPE)_{film}$ ($\mu F\,cm^{-2}$)	n_2
1	0.500	93.02	0.62	0.001	106.5	0.52
3	0.512	104.2	0.64	0.002	111.2	0.58
6	0.661	161.6	0.64	0.002	174.5	0.60
24	0.871	200.2	0.64	0.002	246.7	0.63
48	0.992	210.0	0.64	0.003	322.3	0.63

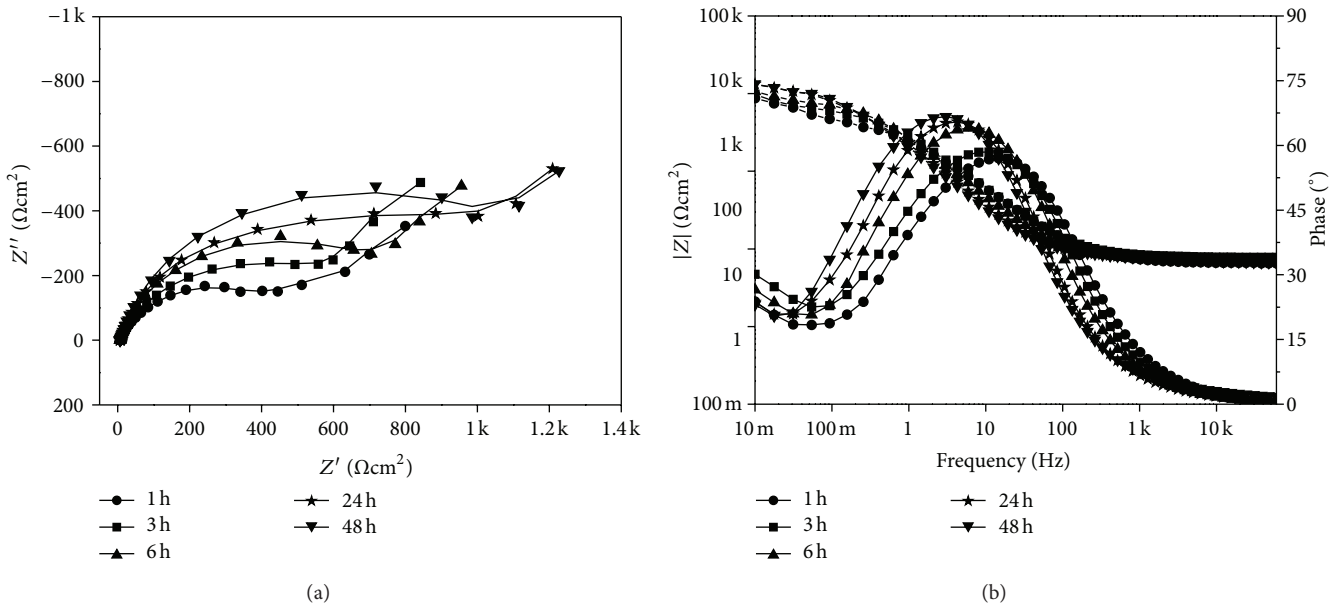

Figure 5: (a) Nyquist and (b) Bode plots of Cu-Ni (90/10) alloy in synthetic seawater polluted with 10 ppm sulphide at different immersion periods. –●–: 1 h, –■–: 3 h, –▲–: 6 h, –★–: 24 h, and –▼–: 48 h. (Temperature: 30°C).

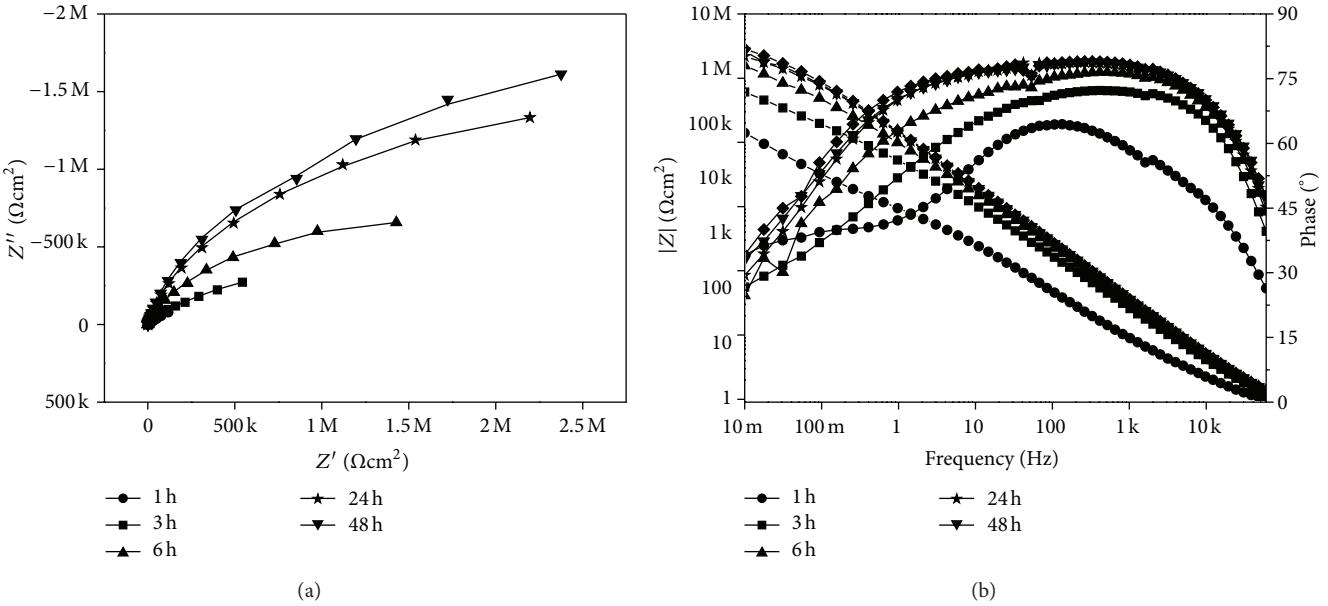

Figure 6: (a) Nyquist and (b) Bode plots of Cu-Ni (90/10) alloy in synthetic seawater polluted with 10 ppm sulphide in the presence of 3.33 mM BTAH at different immersion periods. –●–: 1 h, –■–: 3 h, –▲–: 6 h, –★–: 24 h, and –▼–: 48 h. (Temperature: 30°C).

immersion periods. The Bode plots show some interesting features. There is almost a merger of the plots for different immersion periods at higher frequencies. The phase angle Bode plots showed a clear shift of phase angle maximum towards lower frequencies and broadening of the maximum with the increase in immersion period. However, the phase angle maximum region is narrower in comparison to the corresponding plots in the absence of sulphide. The total impedance Bode plots show the linear behaviour in relatively less range of frequency in the midregion in comparison to the plots in the absence of sulphide ions. The total impedance is also found to be much less in comparison to the system containing no sulphides. Both R_{ct} and R_{film} are increased with the increase in immersion period. But these values are less than those in the absence of sulphides ions in seawater. The $(CPE)_{dl}$ and $(CPE)_{film}$ values are increased in the presence of sulphide ions. That means, by the addition of sulphide ions, the protective nature of the film is reduced. However, both the double layer and the film still show a combination of capacitative and resistive behaviours. Such a large increase in both $(CPE)_{dl}$ and $(CPE)_{film}$ in the presence of only 10 ppm S^{2-} ions shows the significant effect of S^{2-} in modifying especially the inner layer due to the strong specific adsorption of sulphide [32, 33].

Figures 6(a) and 6(b) show the Nyquist and Bode plots of Cu-Ni (90/10) alloy in seawater environment containing 10 ppm of sulphide ions in the presence of 3.33 mM BTAH at different immersion periods. The corresponding impedance parameters are given in Table 8. The Nyquist plots show an increase in both the real and imaginary parts of the complex impedance in the presence of inhibitor. The Bode plots have become much more broadened and the phase angle maxima are increased at all the immersion periods. The phase angle maximum is shifted to much higher frequencies. After 24- and 48-hour immersion periods, the total impedance plots show linearity from the highest frequency of 60 kHz to a low frequency of 10 mHz. All these plots clearly exhibit the capacitative behaviour of both the double layer and of the protective film. Both R_{ct} and R_{film} values are found to increase enormously in the presence of the inhibitor and also with an increase in immersion period. No wonder that the inhibition efficiencies are in the range of 98.81 to 99.97% within the range of immersion period studied. After 48 h immersion period, R_{ct} and the film resistance, respectively, are 2516 and 937.5 kΩ cm^2. The capacitance of the double layer $(CPE)_{dl}$ is reduced from 210.0 μF cm^{-2} to an extremely small value of 0.026 μF cm^{-2} in the presence of BTAH even after 1-hour immersion period. This result indicates the absence of all the ions present in seawater and sulphide ions and presence of only BTAH molecules in the double layer.

Once again the prefilmed alloy is immersed in seawater containing 10 ppm sulphide and 3.33 mM BTAH to investigate the effect of the increase of temperature on the impedance behaviour. The impedance parameters are given in Table 9. Both R_{ct} and R_{film} are reduced with increase in temperature. While $(CPE)_{dl}$ is increased only slightly with the increase in temperature; the increase in $(CPE)_{film}$ is quite significant. Both n_1 and n_2 are reduced to some extent. Nevertheless, the inhibition efficiencies are greater than 99% in the entire temperature range. Thus, impedance studies reveal that BTAH functions quite well as inhibitor in the entire temperature range studied.

3.2. Potentiodynamic Polarization Studies. The potentiodynamic polarization curves for Cu-Ni (90/10) alloy in synthetic seawater in the potential range from −0.7 to +0.7 V versus Ag/AgCl are given in Figure 7 and the corrosion parameters are tabulated in Table 10. The anodic polarization

Table 8: Impedance parameters of Cu-Ni (90/10) alloy in seawater containing 10 ppm of inorganic sulphide in the presence of 3.33 mM BTAH at different immersion periods. (Temperature: 30°C).

Immersion period (h)	R_{ct} (kΩ cm^2)	$(CPE)_{dl}$ (μF cm^{-2})	n_1	R_{film} (kΩ cm^2)	$(CPE)_{film}$ (μF cm^{-2})	n_2	IE (%)
1	42.13	0.577	0.61	8.399	1.621	0.64	98.81
3	390.1	0.086	0.81	47.98	0.602	0.74	99.87
6	712.0	0.043	0.82	114.6	0.476	0.77	99.91
24	1361.0	0.028	0.88	686.2	0.438	0.77	99.94
48	2516.0	0.026	0.90	937.5	0.239	0.82	99.97

Table 9: Impedance parameters of Cu-Ni (90/10) alloy in seawater containing 10 ppm of inorganic sulphide and prefilmed alloy in the presence of 3.33 mM BTAH in seawater containing 10 ppm of inorganic sulphide at different temperatures. (Immersion period: 48 h).

Specimen	Environment	Temperature	R_{ct} (kΩ cm^2)	$(CPE)_{dl}$ (μF cm^{-2})	n_1	R_{film} (kΩ cm^2)	$(CPE)_{film}$ (μF cm^{-2})	n_2	IE (%)
Bare alloy	Seawater + 10 ppm sulphide	40	0.390	168.8	0.58	0.002	434.6	0.57	—
Prefilmed alloy	Seawater + 10 ppm sulphide + 3.33 mM BTAH	40	612.7	0.788	0.79	250.9	0.920	0.73	99.94
Bare alloy	Seawater + 10 ppm sulphide	60	0.184	256.1	0.54	0.002	525.6	0.54	—
Prefilmed alloy	Seawater + 10 ppm sulphide 3.33 mM BTAH	60	398.8	1.033	0.73	223.5	2.621	0.76	99.95

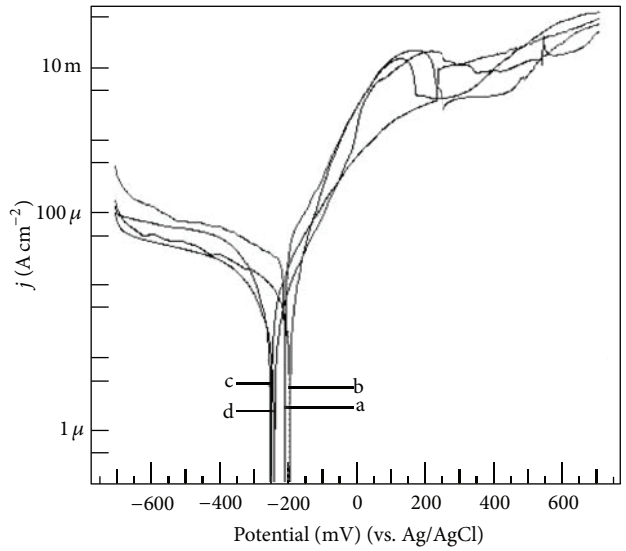

Figure 7: Potentiodynamic polarization curves of Cu-Ni (90/10) alloy in synthetic seawater at different immersion periods. a: 1 h, b: 12 h, c: 24 h, and d: 48 h. (Temperature: 30°C).

curves show three distinct regions, namely, Tafel region at lower overpotentials extending to the peak current density due to the dissolution of copper to Cu^+ ions, a region of decreasing current density until a minimum (i_{min}) is reached due to the formation of CuCl, and a region of the sudden increase in current density leading to a limiting value (i_{lim}), due to the formation of $CuCl_2^-$. These three regions have been reported in the literature in the polarization curves of copper in 3.5% sodium chloride solution [34] and also in the case of Cu-Ni (90/10) alloy [35]. With the increase in immersion period from 1 to 48 h, the corrosion potential (E_{corr}) is shifted towards more negative value and the shift in cathodic Tafel slope (β_c) is greater than the shift in anodic slope (β_a). However, the corrosion current density (i_{corr}) is found to decrease significantly up to 12-hour immersion period and then increase slightly up to 48 h. These results infer that with the increase in immersion period from 1 to 48 h, there is a decrease in the corrosion rate of the alloy due to the formation of copper oxide film, and this has been reported by many investigators [7, 36–38]. Another interesting feature is that while there is only one anodic peak after 1- and 12-hour immersion periods, there are two anodic peaks after 24- and 48-hour immersion periods at 150 and 250 mV versus Ag/AgCl electrode, respectively. The larger peak at 150 mV is

Table 10: Corrosion parameters of Cu-Ni (90/10) alloy obtained by potentiodynamic polarization studies in seawater in the absence of BTAH at different immersion periods. (Temperature: 30°C).

Immersion period (h)	E_{corr} (mV)	i_{corr} (μA cm^{-2})	β_c (mV dec^{-1})	β_a (mV dec^{-1})
1	−219.0	23.3	−165.0	86.8
12	−239.1	4.98	−105.0	90.8
24	−241.0	4.25	−78.1	84.8
48	−251.3	5.98	−115.0	68.2

Table 11: Corrosion parameters of Cu-Ni (90/10) alloy obtained by potentiodynamic polarization studies in seawater in the presence of different concentrations of BTAH at 48-hour immersion period. (Temperature: 30°C).

Concentration of BTAH (mM)	E_{corr} (mV)	i_{corr} (μA cm^{-2})	β_c (mV dec^{-1})	β_a (mV dec^{-1})	IE (%)
0	−251.3	5.98	−115.0	68.2	—
0.82	−217.9	0.141	−95.0	124.0	97.64
1.67	−173.4	0.056	−60.5	81.8	99.06
2.50	−141.4	0.043	−85.2	103.0	99.28
3.33	−117.4	0.042	−70.4	83.7	99.30

Table 12: Corrosion parameters of Cu-Ni (90/10) alloy obtained by potentiodynamic polarization studies in seawater in the presence of 3.33 mM BTAH at different immersion periods. (Temperature: 30°C).

Immersion period (h)	E_{corr} (mV)	i_{corr} (μA cm^{-2})	β_c (mV dec^{-1})	β_a (mV dec^{-1})	IE (%)
1	−207.7	0.128	−96.1	97.6	99.45
12	−210.0	0.070	−74.7	108.0	98.59
24	−195.2	0.067	−81.1	147.0	98.42
48	−117.4	0.042	−70.4	83.7	99.30

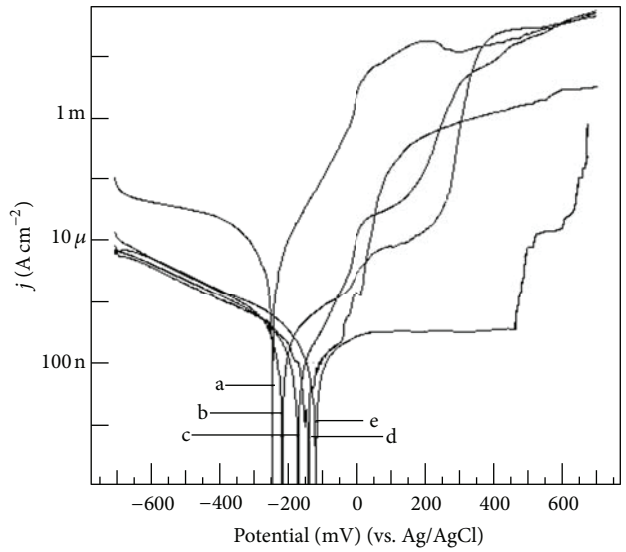

Figure 8: Potentiodynamic polarization curves of Cu-Ni (90/10) alloy in synthetic seawater in the presence of different concentrations of BTAH at 48-hour immersion period. a: 0 mM, b: 0.82 mM, c: 1.67 mM, d: 2.50 mM, and e: 3.33 mM. (Temperature: 30°C).

due to the oxidation of Cu to Cu^+ ions and the smaller peak at 250 mV is due to the oxidation of Cu^+ to Cu^{2+} ions.

The effect of the addition of different concentrations of BTAH to seawater on the corrosion rate of the alloy at a fixed immersion period of 48 h is shown in Figure 8. It is interesting to note that with the addition of the inhibitor, E_{corr} is shifted to a less negative value and as the concentration of inhibitor is increased, E_{corr} is shifted to less and less negative values. However, there is a shift in both the anodic and cathodic Tafel slopes, which indicates that BTAH functions as a mixed inhibitor. The corrosion current density is significantly reduced even with the addition of 0.82 mM BTAH and it decreases further with an increase in the concentration of the inhibitor to 2.50 mM and then remains almost the same at 3.33 mM. Another significant effect is on anodic peaks in the presence of the inhibitor. The two characteristic anodic peaks appeared in the absence of inhibitor are practically absent in the presence of inhibitor. The current density values in the entire anodic region are greatly reduced in the presence of the inhibitor in comparison to the decrease in current densities in the cathodic region. Another interesting feature is to be noted in the anodic polarization curve at 3.33 mM concentration of the inhibitor. The anodic region up to +500 mV versus Ag/AgCl has become passive with extremely low current densities of <1 μA cm^{-2}. It may be noted that the passivity breaks down at a potential >500 mV versus Ag/AgCl. The corrosion parameters are given in Table 11. The inhibition efficiencies calculated using (5) are found to be in the range of 99.30 to 97.64% within the concentration range studied:

$$\text{IE } (\%) = \left(\frac{i_{corr} - i^1_{corr}}{i_{corr}} \right) \times 100. \quad (5)$$

In (5), i_{corr} and i^1_{corr} are the corrosion current densities of Cu-Ni (90/10) alloy in synthetic seawater in the absence and presence of BTAH, respectively.

The potentiodynamic polarization curves of the alloy in seawater in the presence of 3.33 mM of BTAH at different immersion periods are depicted in Figure 9. The corrosion parameters are shown in Table 12. It is interesting to note that the protective nature of the film is evident after 1-hour immersion period itself by a large reduction in corrosion current density from 5.98 to 0.128 μA cm^{-2} and a passive anodic region up to +400 mV versus Ag/AgCl with a small current density of the order of 1 μA cm^{-2}. Nevertheless, with the increase in immersion period up to 48 h, i_{corr} is further reduced to 0.042 μA cm^{-2} and the passive anodic region is extended up to +500 mV versus Ag/AgCl. E_{corr} is shifted to less negative potentials with the increase in immersion period. There is a shift in both the anodic and cathodic Tafel slopes. BTAH shifts E_{corr} from −207.7 mV versus Ag/AgCl after 1-hour immersion period to a less negative potential of

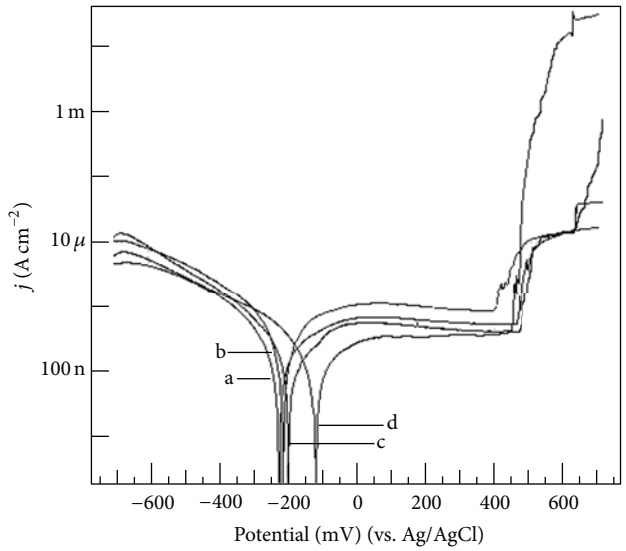

Figure 9: Potentiodynamic polarization curves of Cu-Ni (90/10) alloy in synthetic seawater in the presence of 3.33 mM BTAH at different immersion periods. a: 1 h, b: 12 h, c: 24 h, and d: 48 h. (Temperature: 30°C).

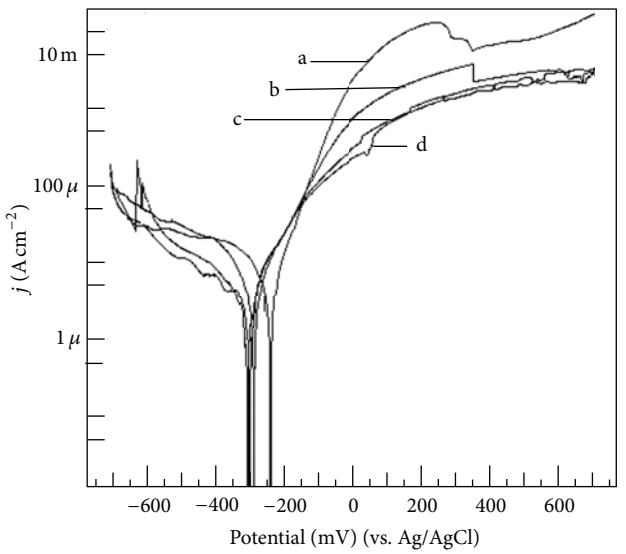

Figure 10: Potentiodynamic polarization curves of Cu-Ni (90/10) alloy in synthetic seawater polluted with 10 ppm sulphide at different immersion periods. a: 1 h, b: 12 h, c: 24 h, and d: 48 h. (Temperature: 30°C).

−117.4 mV versus Ag/AgCl after 48-hour immersion period. This can be possibly interpreted by the inhibitive effect on the anodic reaction of the protective film in terms of the mixed potential theory [39]. Similar behaviour was presented by Allam and Ashour in the case of Cu-Ni (90/10) alloy in 3.4% sodium chloride +2 ppm sulphide in the presence of different concentrations of benzotriazole [40].

The effect of the addition of 10 ppm sulphide to seawater (in the absence of inhibitor) on the polarization behaviour of the alloy after various immersion periods is shown in Figure 10. The corresponding corrosion parameters are shown in Table 13. The corrosion potential is shifted to more negative potentials by the addition of 10 ppm sulphide and the corrosion current density is somewhat reduced [12, 32, 33]. In the presence of sulphide, there is only one anodic peak after 12-hour immersion period and no anodic peaks are observed after 24- and 48-hour immersion periods. With the increase in immersion time, the shift in β_c is much higher than the shift in β_a. This is due to the depletion of sulphide with the increase in immersion time due to the formation of a thick cuprous sulphide film at the surface [41]. According to De Sanchez and Schiffrin [14] and Kato et al. [42]; the main effect of copper sulphide is to accelerate the charge transfer of oxygen reduction, thereby controlling the reduction current density by a diffusive transport through the liquid layer adjacent to the electrode, and this is manifested as the increase in β_c.

When 3.33 mM BTAH is added to the environment containing seawater in the presence of 10 ppm S^{2-} (Figure 11), the corresponding polarization curves of the alloy at different immersion periods show some interesting features. The corresponding corrosion parameters are shown in Table 14. After 1-hour immersion period itself, the corrosion current density is drastically reduced and E_{corr} is shifted to

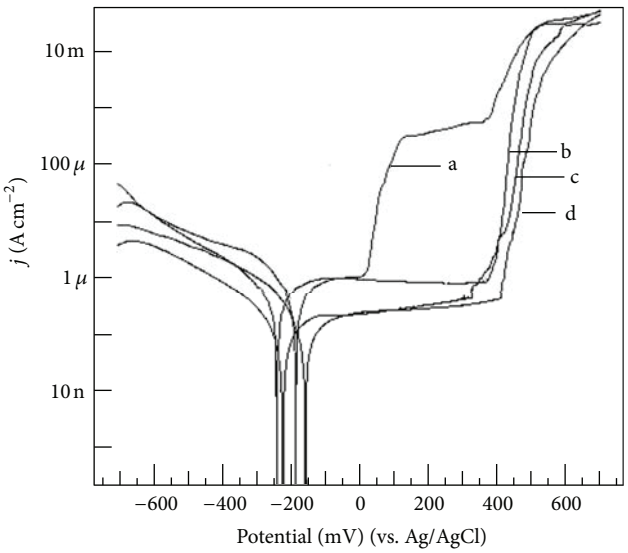

Figure 11: Potentiodynamic polarization curves of Cu-Ni (90/10) alloy in synthetic seawater polluted with 10 ppm sulphide in the presence of 3.33 mM BTAH at different immersion periods. a: 1 h, b: 12 h, c: 24 h, and d: 48 h. (Temperature: 30°C).

less negative potentials. Beyond the Tafel region, there is a passive region up to +10 mV versus Ag/AgCl, and then there is an active region up to +120 mV versus Ag/AgCl, again passive region up to +390 mV versus Ag/AgCl, and finally dissolution leading to limiting current. With the increase in immersion period up to 12 h, the passive region extends from +150 mV to +390 mV and then the dissolution leading to a limiting current. The same trend is observed after 24- and 48-hour immersion times except that there is a further reduction in the corrosion current density. E_{corr} is shifted to more

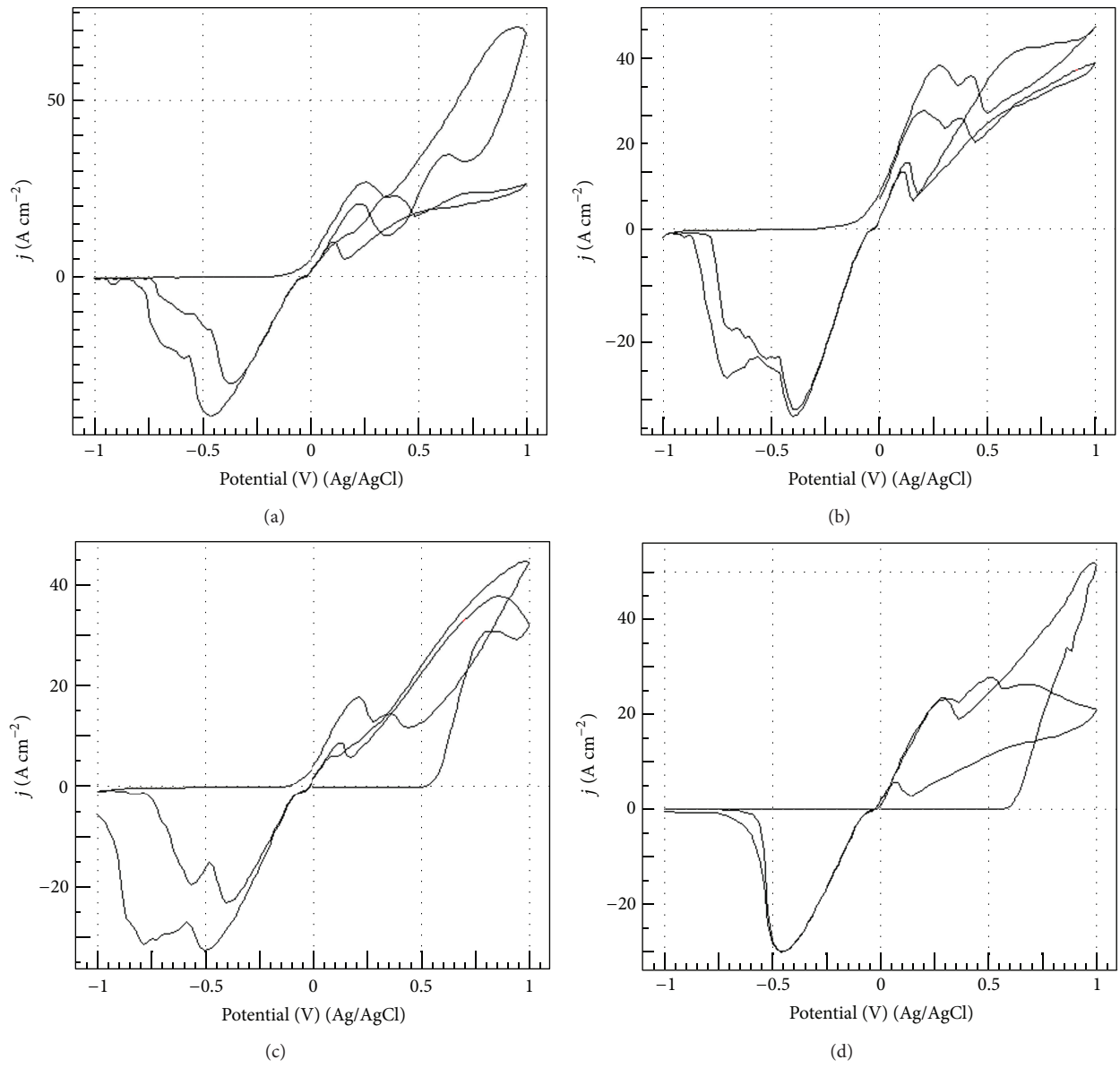

Figure 12: Cyclic voltammograms of Cu-Ni (90/10) alloy in synthetic seawater in the absence ((a): 1 h, (b): 48 h) and presence ((c): 1 h, (d): 48 h) of 3.33 mM BTAH. (Temperature: 30°C).

Table 13: Corrosion parameters of Cu-Ni (90/10) obtained by potentiodynamic polarization studies in seawater containing 10 ppm of inorganic sulphide in the absence of BTAH at different immersion periods. (Temperature: 30°C).

Immersion period (h)	E_{corr} (mV)	i_{corr} (μA cm^{-2})	β_c (mV dec^{-1})	β_a (mV dec^{-1})
1	−239.0	4.27	−138.0	78.0
12	−290.4	3.84	−130.4	81.6
24	−287.6	3.55	−122.0	65.9
48	−303.8	2.77	−191.0	93.4

anodic potentials in the presence of inhibitor at all immersion periods in comparison to the control solution consisting of seawater and 10 ppm sulphide. However, there is a shift in both the anodic and cathodic Tafel slopes, which infer that BTAH acts as a mixed inhibitor. The potentiodynamic polarization studies infer that the corrosion inhibition by BTAH in seawater polluted with 10 ppm sulphide also is more under anodic control.

3.3. Cyclic Voltammetric Studies. The cyclic voltammograms of Cu-Ni (90/10) alloy in seawater in the absence of BTAH in the potential range from −1.0 to +1.0 V versus Ag/AgCl after 1- and 48-hour immersion periods are given in Figures 12(a) and 12(b), respectively. At both immersion periods, in the first cycle, in the forward sweep, they show two anodic peaks. The first peak at +250 mV is due to Cu-Cu$^+$ couple and

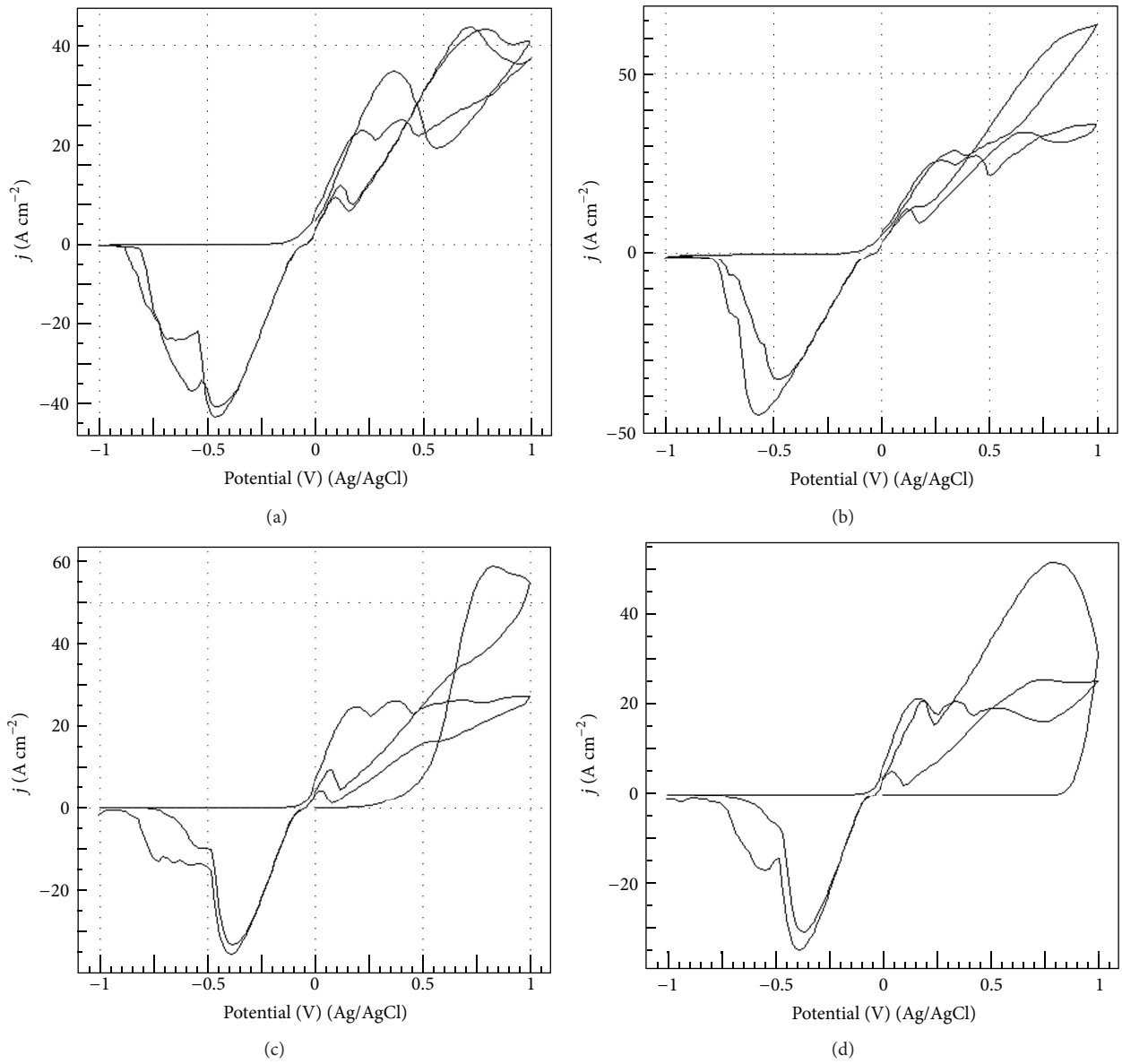

Figure 13: Cyclic voltammograms of Cu-Ni (90/10) alloy in synthetic seawater polluted with 10 ppm sulphide in the absence ((a): 1 h, (b): 48 h) and presence ((c): 1 h, (d): 48 h) of 3.33 mM BTAH. (Temperature: 30°C).

Table 14: Corrosion parameters of Cu-Ni (90/10) alloy obtained by potentiodynamic polarization studies in seawater containing 10 ppm of inorganic sulphide in the presence of 3.33 mM BTAH at different immersion periods. (Temperature: 30°C).

Immersion period (h)	E_{corr} (mV)	i_{corr} (μA cm^{-2})	β_c (mV dec^{-1})	β_a (mV dec^{-1})	IE (%)
1	−182.6	0.308	−119.0	135.0	92.79
12	−238.5	0.189	−88.5	81.8	95.07
24	−224.5	0.047	−76.7	113.0	98.68
48	−157.2	0.032	−45.2	62.6	98.84

the second one at +450 mV is due to Cu^{+}-Cu^{2+} couple. Two corresponding reduction peaks are observed in the reverse sweep. In the second cycle also the same behaviour is seen. Both the anodic and cathodic peak current densities are increased to some extent in the second cycle.

In the presence of 3.33 mM BTAH after 1-hour immersion period (Figure 12(c)), in the first cycle there is no anodic peak up to +500 mV. With the increase in immersion period up to 48 h (Figure 12(d)), the film became more protective even up to +550 mV. In the second cycle, similar

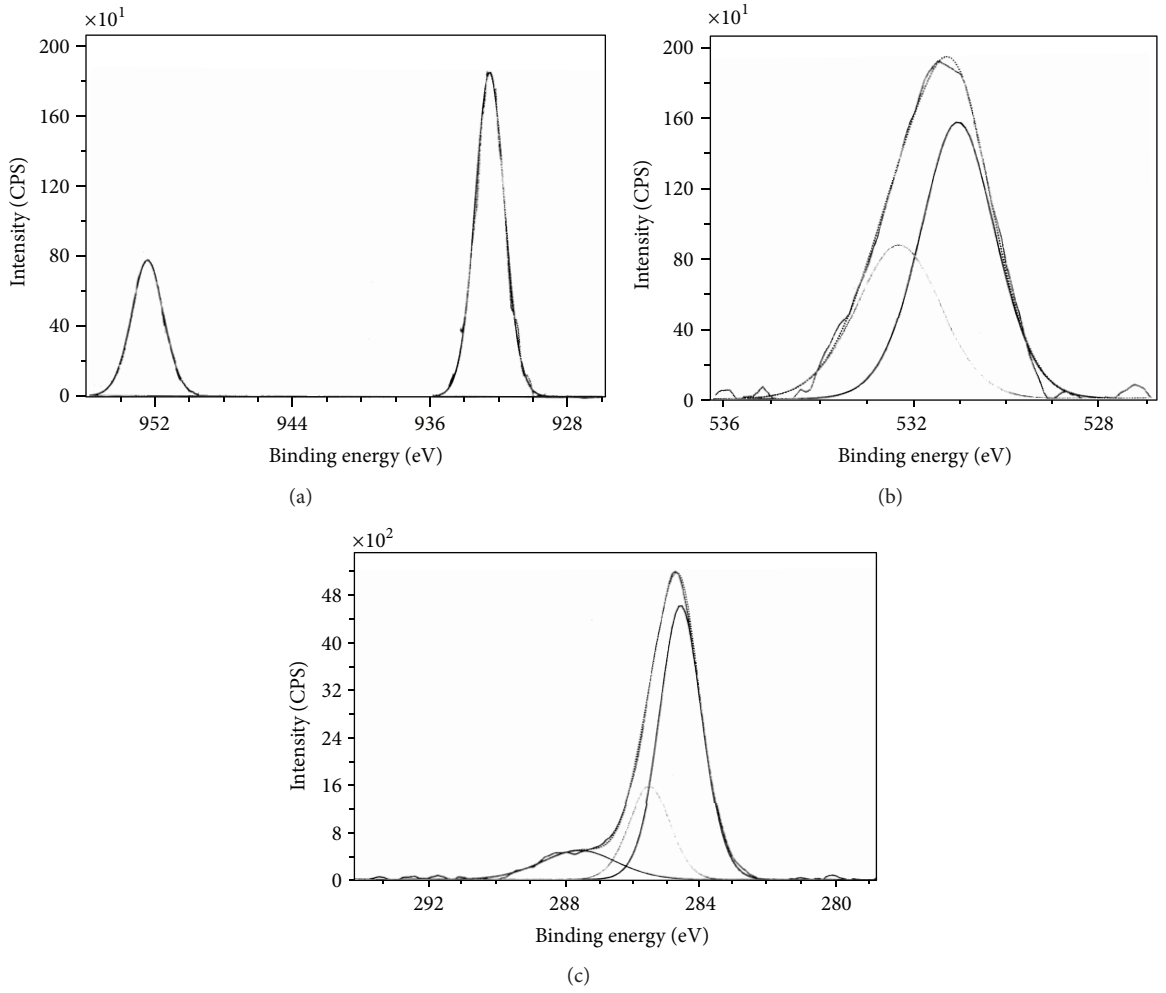

Figure 14: XPS deconvolution spectra of different elements present on the Cu-Ni (90/10) alloy in synthetic seawater in the absence of BTAH for a period of 3 days. ((a): Cu 2p, (b): O 1s, and (c): C 1s).

Table 15: Weight-loss data of Cu-Ni (90/10) alloy in seawater and 10 ppm of inorganic sulphide containing seawater in the absence and presence of different concentrations of BTAH after 30-day immersion period. (Temperature: 30°C).

Environment	Weight before immersion (W_1) (g)	Weight after immersion (W_2) (g)	Weight loss (ΔW) (g)	Corrosion rate (mmpy)	IE (%)
Seawater	8.10845	8.09889	0.00956	0.01295	—
Seawater + 10 ppm sulphide	8.26840	8.25173	0.01667	0.02258	—
Seawater + 2.5 mM BTAH	8.15888	8.15825	0.00063	0.00085	93.41
Seawater + 3.33 mM BTAH	8.56288	8.56283	0.00005	0.00007	99.48
Seawater + 10 ppm sulphide + 2.5 mM BTAH	7.71100	7.70865	0.00235	0.00318	85.90
Seawater + 10 ppm sulphide + 3.33 mM BTAH	8.28198	8.28191	0.00007	0.00009	99.58

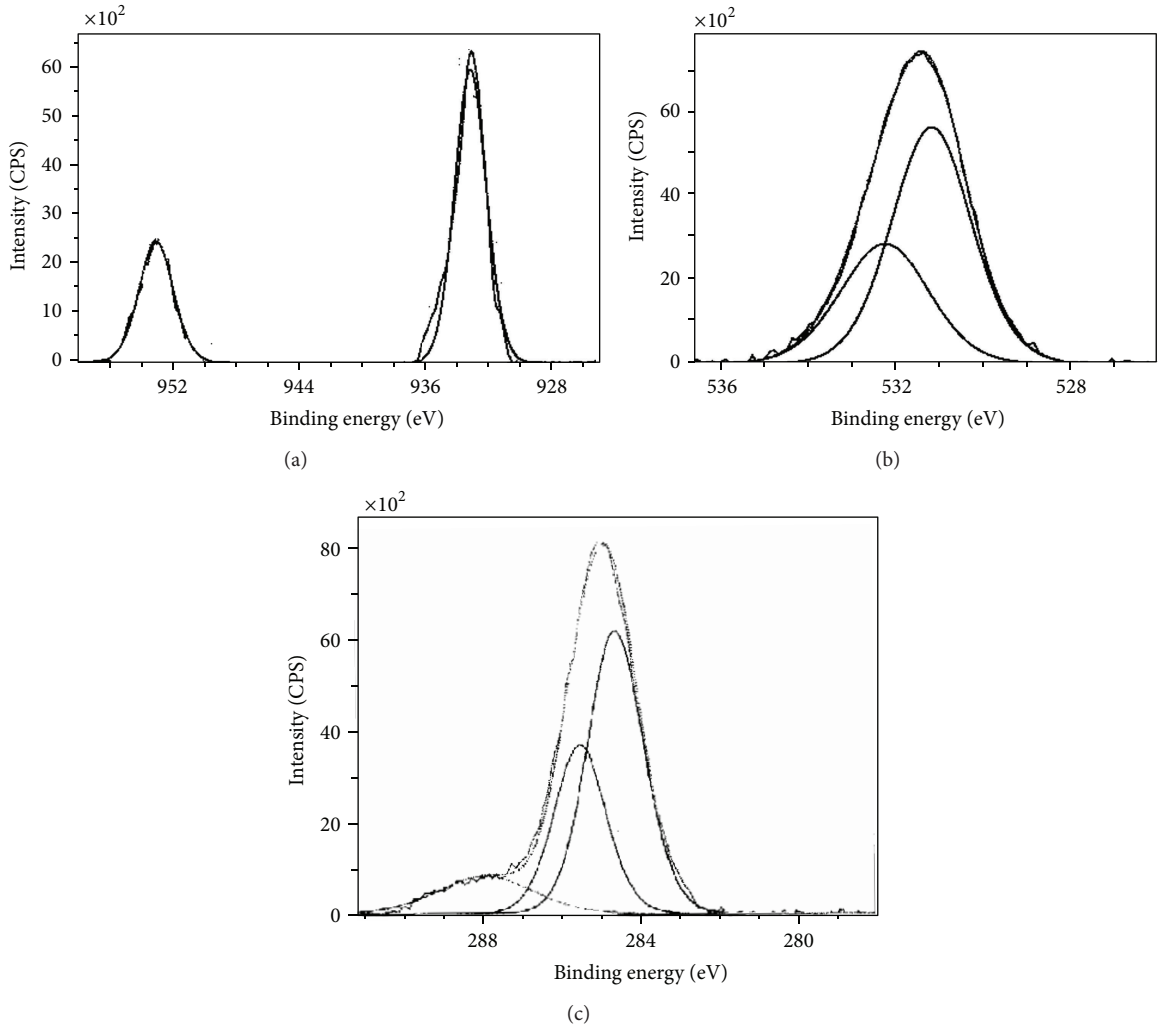

Figure 15: XPS deconvolution spectra of different elements present on the Cu-Ni (90/10) alloy in synthetic seawater containing 10 ppm sulphide in the absence of BTAH for a period of 3 days. ((a): Cu 2p, (b): O 1s, and (c): C 1s).

behaviour of bare alloy in the absence of BTAH is seen because of the breakdown of the film as a consequence of the application of higher potentials up to 1.0 V versus Ag/AgCl. The CV profiles confirm that BTAH inhibitor functions excellently and protects the Cu-Ni (90/10) alloy from corrosion in seawater environment. Similar behaviour is also exhibited in the presence of 10 ppm sulphide-polluted seawater environment, both in the absence (Figures 13(a) and 13(b)) and presence (Figures 13(c) and 13(d)) of BTAH.

3.4. Gravimetric Studies. The results of gravimetric studies of Cu-Ni (90/10) alloy in seawater and 10 ppm sulphide containing seawater in the absence and presence of two different concentrations of BTAH after an immersion period of 30 days are shown in Table 15. The concentrations of BTAH are chosen based on the inhibition efficiencies obtained from electrochemical studies. Essentially these studies are carried out to find out the efficiency of the inhibitor after a long immersion period, such as 30 days. When 2.5 mM BTAH is added to seawater and sulphide-polluted seawater, the corrosion rates are decreased. When the concentration of BTAH is increased to 3.33 mM, negligible weight loss is observed in both the environments. At 3.33 mM concentration of BTAH, an inhibition efficiency of more than 99% is obtained in both seawater and sulphide-polluted seawater environments. Thus, the results of gravimetric studies revealed that the inhibitor, BTAH, proved to be an excellent inhibitor even after an immersion period of 30 days.

3.5. X-Ray Photoelectron Spectroscopic Studies (XPSs). In the XPS survey spectrum of Cu-Ni (90/10) alloy in seawater in the absence of BTAH after 3-day immersion period, the peaks due to copper, oxygen, and carbon are detected. No appreciable nickel signal is seen. The computer deconvolution spectra for copper, oxygen, and carbon are shown in Figures 14(a), 14(b), and 14(c), respectively. The high resolution Cu $2p_{3/2}$ peak at 932.4 eV and Cu $2p_{1/2}$ peak at 952.4 eV are attributed to Cu_2O [43]. The O 1s peak at 531.0 eV is ascribed to the

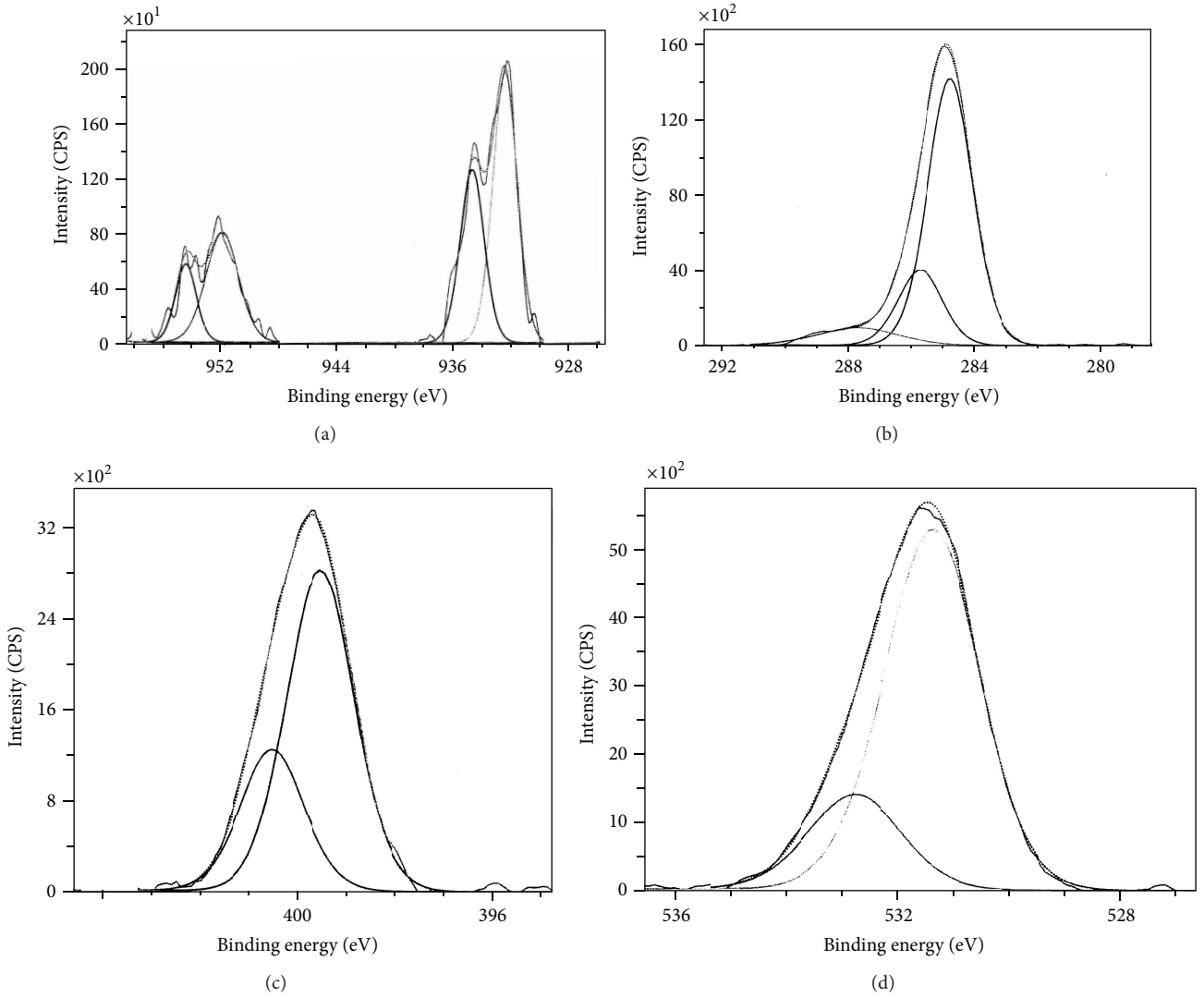

Figure 16: XPS deconvolution spectra of different elements present on the Cu-Ni (90/10) alloy in synthetic seawater in the presence of 3.33 mM BTAH for a period of 3 days. ((a): Cu 2p, (b): C 1s, (c): N 1s, and (d): O 1s).

presence of Cu_2O [44]. The O 1s peak at 532.3 eV is due to the presence of hydroxide [45]. From these observations, it is concluded that the outermost corrosion product is Cu_2O. The C 1s peaks at 284.6 eV, 285.5 eV, and 287.6 eV are due to contaminant carbon, which is likely due to the cracking of vacuum oil used during the operation of XPS instrument [46].

The survey scan of the film formed on Cu-Ni (90/10) alloy in 10 ppm sulphide containing seawater in the absence of BTAH also shows the peaks due to copper, oxygen, and carbon. The computer deconvolution spectra for copper, oxygen, and carbon are shown in Figures 15(a), 15(b), and 15(c), respectively. The sulphur signal is not observed because the sulphide is oxidized by dissolved oxygen in seawater. The half-life of sulphide studied by Bates and Popplewell [47] at a concentration of 3.8 ppm in the air-saturated seawater is of the order of 20 min. Ostland and Alexander [48] investigated that 10 ppm sulphide decayed to 0.1–1.0 ppm after 1 day in the air-saturated seawater. In our present study, the immersion period is 3 days. Hence, the sulphur signal is not detected. The presence of Cu $2p_{3/2}$ peak at 932.9 eV and Cu $2p_{1/2}$ peak at 952.9 eV confirms the presence of Cu (I) [43]. The O 1s peaks at 531.2 eV and 532.2 eV are due to the presence of oxide and hydroxide, respectively. From these observations, it is inferred that in sulphide containing seawater also, the major corrosion product is found to be Cu_2O. The C 1s peaks at 284.6 eV, 285.5 eV, and 287.9 eV are due to contaminant carbon.

The XPS survey spectrum of Cu-Ni (90/10) alloy in seawater in the presence of BTAH after 3-day immersion period shows peaks corresponding to copper, carbon, nitrogen, and oxygen. The corresponding computer deconvolution spectra are shown in Figures 16(a), 16(b), 16(c), and 16(d). The Cu 2p spectrum shows peaks due to Cu $2p_{3/2}$ at 932.2 eV with a satellite peak at 934.5 eV and Cu $2p_{1/2}$ at 952.3 eV with a satellite peak at 954.7 eV. The shake-up satellite structures

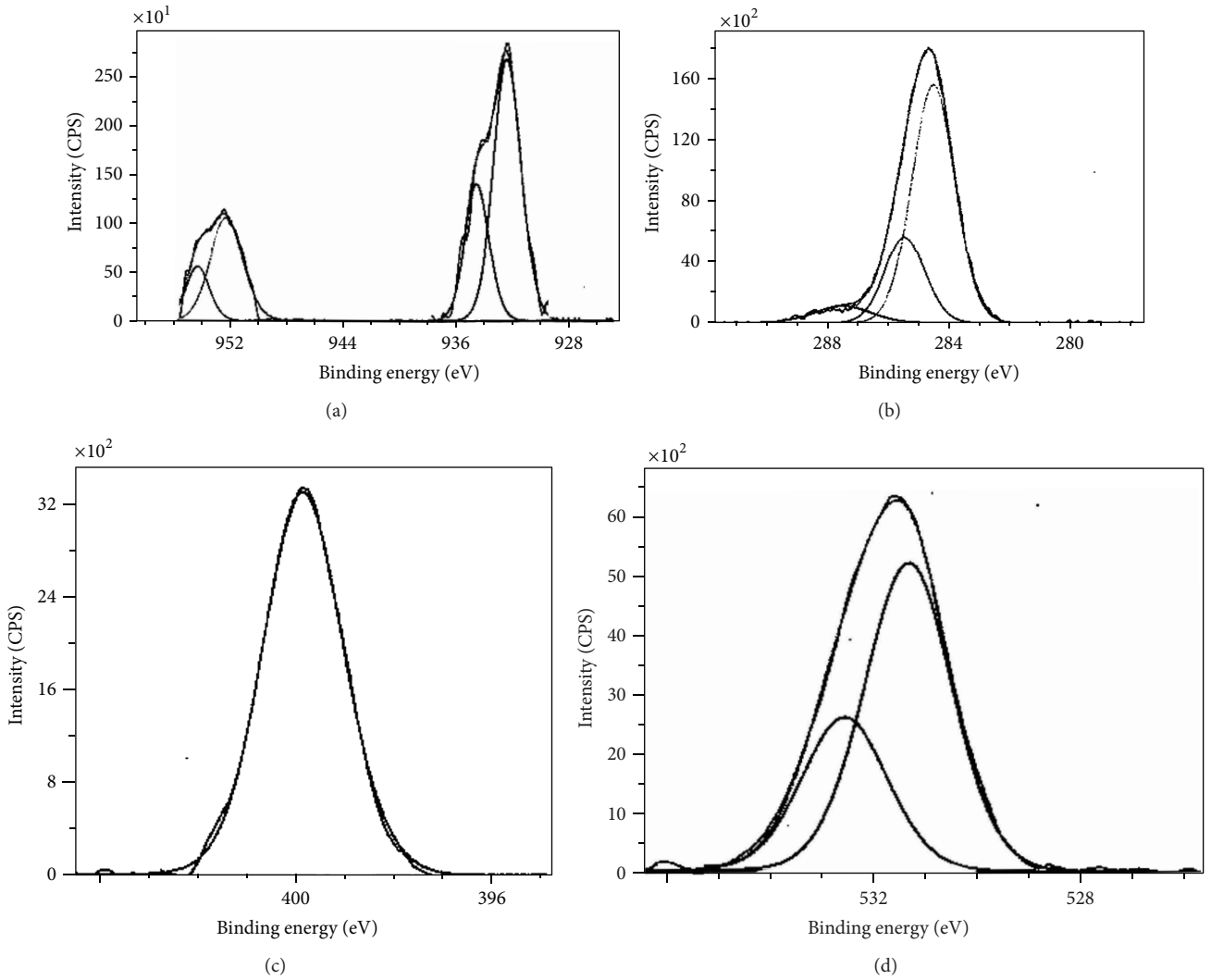

Figure 17: XPS deconvolution spectra of different elements present on the Cu-Ni (90/10) alloy in synthetic seawater containing 10 ppm sulphide in the presence of 3.33 mM BTAH for a period of 3 days. ((a): Cu 2p, (b): C 1s, (c): N 1s, and (d): O 1s).

are closely related to the oxidation state of copper [49]. All cupric compounds whose Cu 2p spectra have been studied show satellite peaks arise due to multielectron excitation process. From these observations, the presence of Cu (II)-BTA complex is inferred. In fact, there is a formation of Cu (I)-BTA complex, which is oxidized to Cu (II)-BTA complex in the course of time. The observed transition from a Cu (I) species to a Cu (II) species is in agreement with the results of studies reported in literature [50, 51]. C 1s shows three peaks, one at 285.6 eV and the other two at 284.6 eV and 287.6 eV. The C 1s peak at 285.6 eV is characteristic of carbon present in aromatic ring [52]. The C 1s peaks at 284.6 eV and 287.6 eV are due to contaminant carbon. N 1s spectrum shows two peaks, one at 399.6 eV and the other at 400.6 eV, which are due to the presence of nitrogen atoms in BTAH in two different chemical environments. The peak at 399.6 eV is assigned to "N=N" group and the one at 400.6 eV is assigned to "HN–N" group. Two O 1s peaks are also observed in the presence of BTAH. This result infers the formation of Cu_2O film over which Cu (I)-BTA complex is formed.

The XPS deconvolution spectra (Figures 17(a), 17(b), 17(c), and 17(d)) of Cu-Ni (90/10) alloy in seawater containing 10 ppm sulphide in the presence of BTAH after 3-day immersion period show peaks corresponding to Cu $2p_{3/2}$, Cu $2p_{1/2}$, C 1s, N 1s, and O 1s. The Cu $2p_{3/2}$ at 932.3 eV associated with a satellite peak at 934.5 eV and the Cu $2p_{1/2}$ at 952.5 eV associated with a satellite peak at 954.6 eV infer the presence of Cu (II)-BTA complex. The C 1s peak at 285.6 eV is characteristic of carbon present in aromatic ring [52]. The C 1s peaks at 284.6 eV and 287.7 eV are due to contaminant carbon. The N 1s peak at 399.8 eV is due to the delocalization of the three nitrogen atoms present in the ring, providing negative charge to the ring. Al Kharafi et al. studied the effect of sulphide pollution on the stability of the protective film of benzotriazole on copper surface [53]. They obtained a single peak at 400.0 eV and interpreted

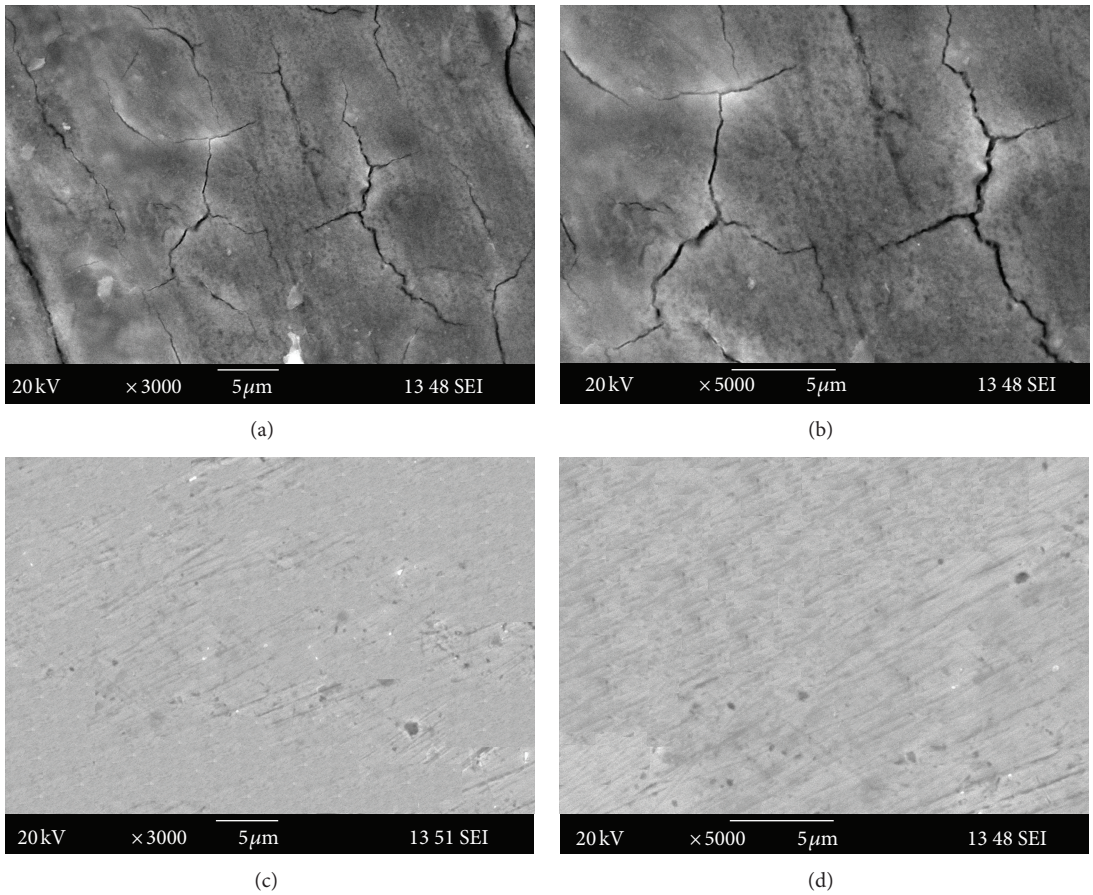

Figure 18: SEM images of Cu-Ni (90/10) alloy in synthetic seawater in the absence ((a): ×3000, (b): ×5000) and presence ((c): ×3000, (d): ×5000) of BTAH for a period of 30 days.

the same to the three nitrogen atoms of the benzotriazole ring. Souto et al. studied the corrosion inhibition of copper by benzotriazole and potassium ethyl xanthate in aqueous solutions containing 0.1 M NaCl [54]. They reported a single N 1s peak due to the presence of benzotriazole on the copper surface.

3.6. Scanning Electron Microscopy (SEM)/Energy Dispersive X-Ray Analysis (EDX). Scanning electron micrographs of Cu-Ni (90/10) alloy in seawater in the absence of BTAH after 30-day immersion at different magnifications are shown in Figure 18(a). The SEM image of Cu-Ni (90/10) alloy in seawater in the absence of BTAH clearly shows that the surface is severely corroded and there is a formation of different forms of corrosion products on the alloy surface. Breakdown of oxide film is also seen. To increase the aggressiveness of the environment, 10 ppm of inorganic sulphide is added to seawater (Figure 19(a)). In this environment, the corrosion damage on the alloy surface is relatively more severe. The entire surface is covered by a scale-like black corrosion product. However, in the presence of BTAH in both seawater (Figure 18(b)) and sulphide containing seawater (Figure 19(b)), the surface is smooth with small notches. These micrographs reveal the absence of any corrosion product.

The EDX spectra in the absence of BTAH in seawater (Figure 20(a)) confirm the presence of a large amount of Cu_2O as indicated by the very high intensity of O signal. In sulphide-polluted seawater (Figure 21(a)), in addition to O signal, S signal is also detected. Hence, it confirms that the corrosion products are both Cu_2O and Cu_2S in sulphide-polluted seawater. However, in the presence of BTAH in both seawater (Figure 20(b)) and sulphide-polluted seawater (Figure 21(b)), the spectra show signals, which are characteristic of the existence of C and N present in the BTAH molecule. In addition, the intensity of O signal is significantly reduced. The S signal is completely absent in sulphide-polluted seawater in the presence of BTAH. The EDX spectra indicate the presence of protective BTAH film on alloy surface. The elemental composition of Cu-Ni (90/10) alloy obtained during all these studies is given in Table 16.

4. Conclusions

(1) All the three electrochemical methods reveal that 1,2,3-benzotriazole is proved to be an excellent inhibitor for Cu-Ni (90/10) alloy in synthetic seawater and seawater containing sulphide ions.

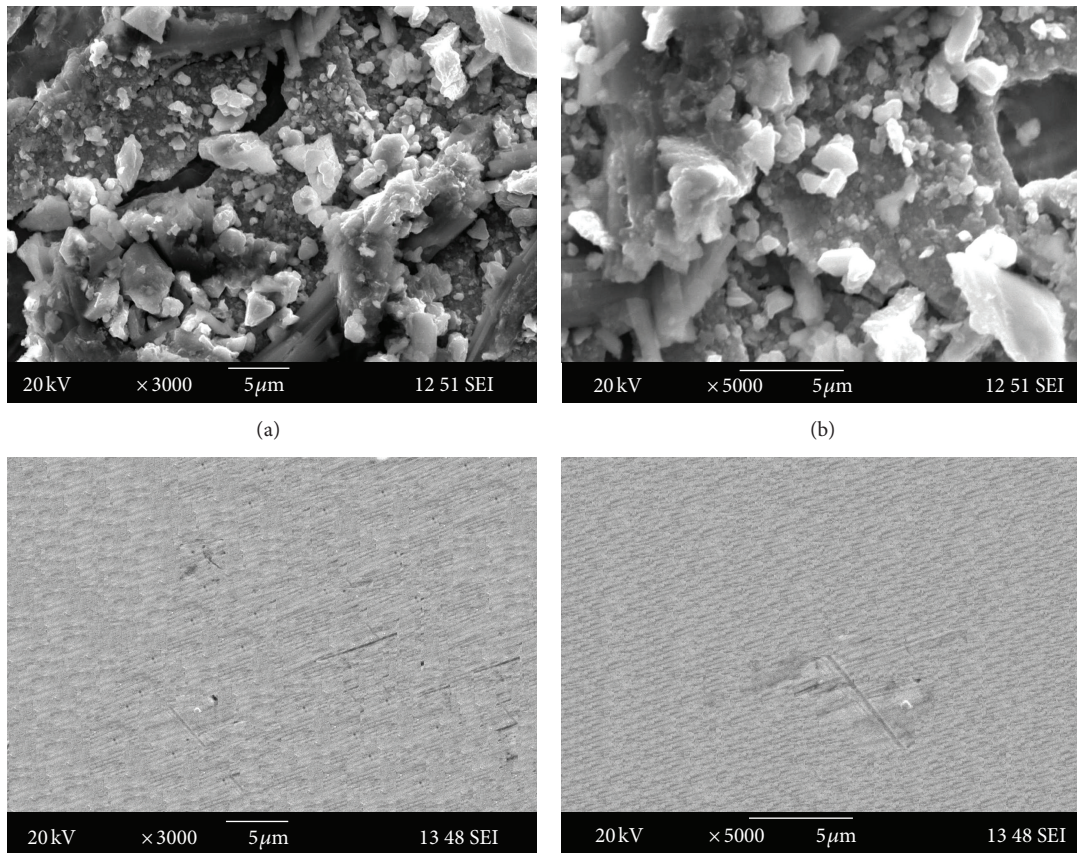

Figure 19: SEM images of Cu-Ni (90/10) alloy in synthetic seawater containing 10 ppm sulphide in the absence ((a): ×3000, (b): ×5000) and presence ((c): ×3000, (d): ×5000) of BTAH for a period of 30 days.

Table 16: Elemental composition of Cu-Ni (90/10) alloy obtained by SEM-EDX in seawater and sulphide-polluted seawater in the absence and presence of BTAH after 30-day immersion period.

Seawater		Seawater + 10 ppm sulphide		Seawater + 3.33 mM BTAH		Seawater + 10 ppm sulphide + 3.33 mM BTAH	
Element	Atom (%)	Element	Atom (%)	Element	Atom (%)	Element	Atom (%)
O	54.5	O	39.37	C K	30.47	C K	28.58
S	0.6	S	17.34	N K	4.14	N K	3.25
Cl	1.29	Cl	2.02	O K	2.64	O K	6.51
Fe	0.97	Fe	0.56	Fe K	0.85	Fe K	0.87
Ni	6.17	Ni	4.59	Ni K	7.1	Ni K	7.81
Cu	36.47	Cu	36.12	Cu K	54.8	Cu K	52.98

(2) BTAH is proved to be an excellent inhibitor even after an immersion period of 30 days, as evidenced by weight-loss studies.

(3) Electrochemical impedance studies showed that BTAH molecules increase both the charge transfer resistance and the film resistance of the Cu-Ni (90/10) alloy. The protective BTAH film withstands even up to 60°C.

(4) Potentiodynamic polarization studies indicated that BTAH considerably shifts the corrosion potential to less negative values and greatly decreases the corrosion current density. These studies give valuable information regarding the anodic behavior of Cu-Ni (90/10) alloy in the absence and presence of BTAH, which is proved to be a mixed inhibitor, predominantly anodic in nature.

(5) Cyclic voltammeric studies show the stability of the protective film even at anodic potentials of 550 mV versus Ag/AgCl.

(6) Surface examination studies by XPS and SEM-EDX confirm the presence of protective BTAH film on the alloy surface.

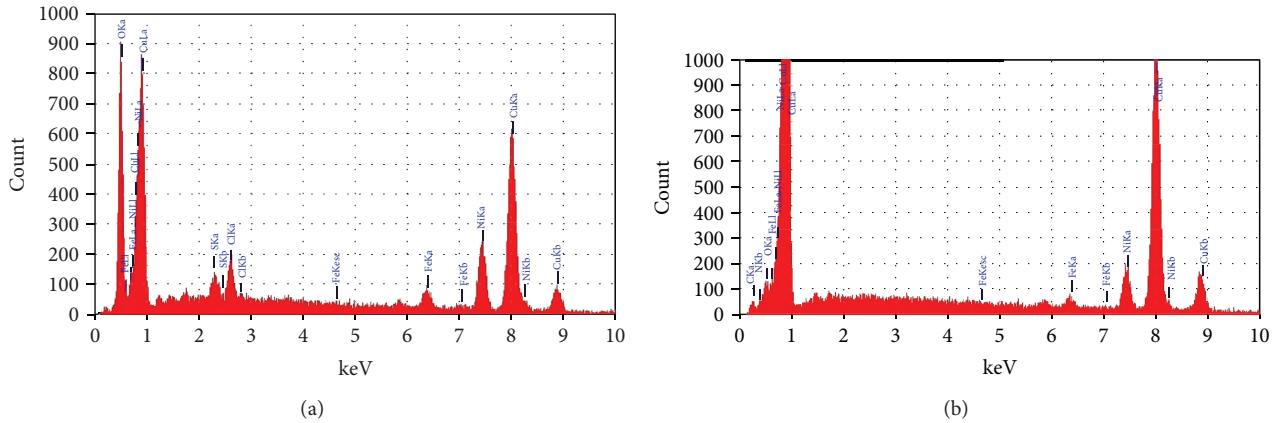

Figure 20: EDX spectra of Cu-Ni (90/10) alloy in synthetic seawater in the (a) absence and (b) presence of BTAH for a period of 30 days.

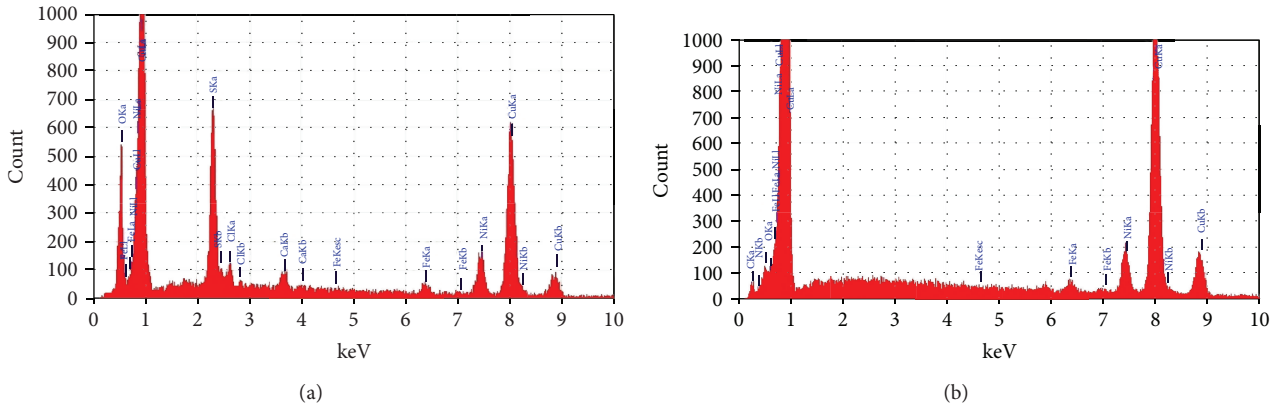

Figure 21: EDX spectra of Cu-Ni (90/10) alloy in synthetic seawater containing 10 ppm sulphide in the (a) absence and (b) presence of BTAH for a period of 30 days.

Acknowledgments

The authors are grateful to Naval Research Board (NRB), Government of India and Rajiv Gandhi National Fellowship (RGNF), UGC, Government of India for giving the financial assistance.

References

[1] R. W. Cahn, P. Hassen, and E. J. Kramer, *Materials Science and Technology, A Comprehensive Treatment, Structure and Properties of Non-Ferrous Alloys*, vol. 8, VCH, New York, NY, USA, 1996.

[2] E. G. West, *Copper and Its Alloys*, Ellis Horwood Ltd., Halsted Press, New York, NY, USA, 1982.

[3] B. Todd and P. A. Lovett, "Marine engineering practice: selecting materials for seawater systems," Tech. Rep., Institute of Marine Engineers, London, UK, 1976.

[4] C. A. Powell, "Marine applications of copper-nickel alloys, section 1: copper-nickel alloys-resistance to corrosion and biofouling," Tech. Rep., Copper Development Association, Potters Bar, UK, 1998.

[5] F. Mansfeld and B. J. Little, "Microbiologically influenced corrosion of copperbased materials exposed to natural seawater," *Electrochimica Acta*, vol. 37, no. 12, pp. 2291–2297, 1992.

[6] A. Hall and A. J. M. Baker, "Settlement and growth of copper-tolerant *Ectocarpus siliculosus* (Dillw.) Lyngbye on different copper-based antifouling surfaces under laboratory conditions," *Journal of Material Science*, vol. 20, no. 3, pp. 1111–1118, 1985.

[7] C. Kato, B. G. Ateya, J. E. Castle, and H. W. Pickering, "On the mechanism of corrosion of Cu-9.4Ni-1.7Fe alloy in air saturated aqueous NaCl solution—I. Kinetic investigations," *Journal of the Electrochemical Society*, vol. 127, no. 9, pp. 1890–1896, 1980.

[8] S. Cere and M. Vazquez, "Properties of the passive films present on copper and copper-nickel alloys in slightly alkaline solutions," *Journal of Materials Science Letters*, vol. 21, no. 6, pp. 493–495, 2002.

[9] J. O. M. Bockris, B. T. Rubin, A. Despic, and B. Lovrecek, "The electrodissolution of coppernickel alloys," *Electrochimica Acta*, vol. 17, no. 5, pp. 973–999, 1972.

[10] R. F. North and M. J. Pryor, "The influence of corrosion product structure on the corrosion rate of Cu-Ni alloys," *Corrosion Science*, vol. 10, no. 5, pp. 297–311, 1970.

[11] T. D. Burleigh and D. H. Waldeck, "Effect of alloying on the resistance of Cu-10% Ni alloys to seawater impingement," *Corrosion*, vol. 55, no. 8, pp. 800–804, 1999.

[12] S. M. Sayed, E. A. Ashour, and G. I. Youssef, "Effect of sulfide ions on the corrosion behaviour of Al-brass and Cu10Ni alloys

in salt water," *Materials Chemistry and Physics*, vol. 78, no. 3, pp. 825–834, 2003.

[13] H. Hack, "Susceptibility of 17 machinery alloys to sulphide induced corrosion in seawater," Tech. Rep. AWFAL-TR-B1-4019, Bethesda, Md, USA, 1980.

[14] S. R. De Sanchez and D. J. Schiffrin, "The flow corrosion mechanism of copper base alloys in sea water in the presence of sulphide contamination," *Corrosion Science*, vol. 22, no. 6, pp. 585–607, 1982.

[15] M. Benmessaoud, K. Es-salah, N. Hajjaji, H. Takenouti, A. Srhiri, and M. Ebentouhami, "Inhibiting effect of 2-mercaptobenzimidazole on the corrosion of Cu-30Ni alloy in aerated 3% NaCl in presence of ammonia," *Corrosion Science*, vol. 49, no. 10, pp. 3880–3888, 2007.

[16] W. A. Badawy, K. M. Ismail, and A. M. Fathi, "Environmentally safe corrosion inhibition of the Cu-Ni alloys in acidic sulfate solutions," *Journal of Applied Electrochemistry*, vol. 35, no. 9, pp. 879–888, 2005.

[17] E. M. M. Sutter, F. Ammeloot, M. J. Pouet, C. Fiaud, and R. Couffignal, "Heterocyclic compounds used as corrosion inhibitors: correlation between ^{13}C and 1H NMR spectroscopy and inhibition efficiency," *Corrosion Science*, vol. 41, no. 1, pp. 105–115, 1999.

[18] D. Tromans and R. H. Sun, "Anodic polarization behavior of copper in aqueous chloride/benzotriazole solutions," *Journal of the Electrochemical Society*, vol. 138, no. 11, pp. 3235–3244, 1991.

[19] I. H. Omar, F. Zucchi, and G. Trabanelli, "Schiff bases as corrosion inhibitors of copper and its alloys in acid media," *Surface and Coatings Technology*, vol. 29, no. 2, pp. 141–151, 1986.

[20] W. A. Badawy, K. M. Ismail, and A. M. Fathi, "Corrosion control of Cu-Ni alloys in neutral chloride solutions by amino acids," *Electrochimica Acta*, vol. 51, no. 20, pp. 4182–4189, 2006.

[21] R. Babic, M. Metikos-Hukovic, and M. Loncar, "Impedance and photoelectrochemical study of surface layers on Cu and Cu-10Ni in acetate solution containing benzotriazole," *Electrochimica Acta*, vol. 44, no. 14, pp. 2413–2421, 1999.

[22] N. K. Allam, E. A. Ashour, H. S. Hegazy, B. E. El-Anadouli, and B. G. Ateya, "Effects of benzotriazole on the corrosion of Cu10Ni alloy in sulfide-polluted salt water," *Corrosion Science*, vol. 47, no. 9, pp. 2280–2292, 2005.

[23] J. M. Maciel and S. M. L. Agostinho, "Use of a rotating cylinder electrode in corrosion studies of a 90/10 Cu-Ni alloy in 0.5 mol L^{-1} H_2SO_4 media," *Journal of Applied Electrochemistry*, vol. 30, no. 8, pp. 981–985, 2000.

[24] S. J. Yuan and S. O. Pehkonen, "Surface characterization and corrosion behavior of 70/30 CuNi alloy in pristine and sulfide-containing simulated seawater," *Corrosion Science*, vol. 49, no. 3, pp. 1276–1304, 2007.

[25] ASTM Standard G 31-72, *Standard Practice for Laboratory Immersion Corrosion Testing of Metals*, Annual Book of ASTM Standards, ASTM, Philadelphia, Pa, USA, 1990.

[26] R. A. Freeman and D. C. Silverman, "Error propagation in coupon immersion tests," *Corrosion*, vol. 48, no. 6, pp. 463–466, 1992.

[27] A. L. Bacarella and J. C. Griess, "The anodic dissolution of copper in flowing sodium chloride solutions between 25° and 175°C," *Journal of the Electrochemical Society*, vol. 120, no. 4, pp. 459–465, 1973.

[28] G. Kear, B. D. Barker, and F. C. Walsh, "Electrochemical corrosion of unalloyed copper in chloride media—a critical review," *Corrosion Science*, vol. 46, no. 1, pp. 109–135, 2004.

[29] F. Bentiss, M. Lagrenee, M. Traisnel, and J. C. Hornez, "The corrosion inhibition of mild steel in acidic media by a new triazole derivative," *Corrosion Science*, vol. 41, no. 4, pp. 789–803, 1999.

[30] Y. S. Tan, M. P. Srinivasan, S. O. Pehkonen, and S. Y. M. Chooi, "Effects of ring substituents on the protective properties of self-assembled benzenethiols on copper," *Corrosion Science*, vol. 48, no. 4, pp. 840–862, 2006.

[31] X. Wu, H. Ma, S. Chen, Z. Xu, and A. Sui, "General equivalent circuits for faradaic electrode processes under electrochemical reaction control," *Journal of the Electrochemical Society*, vol. 146, no. 5, pp. 1847–1853, 1999.

[32] B. C. Syrett, "The mechanism of accelerated corrosion of coppernickel alloys in sulphidepolluted seawater," *Corrosion Science*, vol. 21, no. 3, pp. 187–209, 1981.

[33] L. E. Eiselstein, B. C. Syrett, S. S. Wing, and R. D. Caligiuri, "The accelerated corrosion of Cu-Ni alloys in sulphide-polluted seawater: mechanism no. 2," *Corrosion Science*, vol. 23, no. 3, pp. 223–239, 1983.

[34] E. M. Sherif, R. M. Erasmus, and J. D. Collins, "Inhibition of corrosion processes on copper in aerated sodium chloride solutions by 5-(3-aminophenyl)-tetrazole," *Journal of Applied Electrochemistry*, vol. 39, no. 1, pp. 83–91, 2009.

[35] A. M. Alfantazi, T. M. Ahmed, and D. Tromans, "Corrosion behavior of copper alloys in chloride media," *Materials and Design*, vol. 30, no. 7, pp. 2425–2430, 2009.

[36] Y. Z. Wang, A. M. Beccaria, and G. Poggi, "The effect of temperature on the corrosion behaviour of a 70/30 Cu-Ni commercial alloy in seawater," *Corrosion Science*, vol. 36, no. 8, pp. 1277–1288, 1994.

[37] P. Druska, H. H. Strehblow, and S. Golledge, "A surface analytical examination of passive layers on Cu-Ni alloys—part I. Alkaline solution," *Corrosion Science*, vol. 38, no. 6, pp. 835–851, 1996.

[38] J. M. Popplewell, R. J. Hart, and J. A. Ford, "The effect of iron on the corrosion characteristics of 90-10 cupro nickel in quiescent 3.4% NaCl solution," *Corrosion Science*, vol. 13, no. 4, pp. 295–309, 1973.

[39] W. S. Tait, *An Introduction to Electrochemical Corrosion Testing for Practicing Engineers and Scientists*, University of Wisconsin, Madison, Wis, USA, 1994.

[40] N. K. Allam and E. A. Ashour, "Promoting effect of low concentration of benzotriazole on the corrosion of Cu10Ni alloy in sulfide polluted salt water," *Applied Surface Science*, vol. 254, no. 16, pp. 5007–5011, 2008.

[41] J. N. Al-Hajji and M. R. Reda, "On the effects of common pollutants on the corrosion of copper-nickel alloys in sulfide polluted seawater," *Journal of Electrochemical Society*, vol. 142, no. 9, pp. 2944–2953, 1995.

[42] C. Kato, H W. Pickering, and J. E. Castle, "Effect of sulfide on the corrosion of Cu-9.4Ni-1.7Fe Alloy in aqueous NaCl solution," *Journal of Electrochemical Society*, vol. 131, no. 6, pp. 1225–1229, 1984.

[43] N. S. Mclntyre and M. G. Cook, "X-ray photoelectron studies on some oxides and hydroxides of cobalt, nickel and copper," *Analytical Chemistry*, vol. 47, no. 13, pp. 2208–2213, 1975.

[44] N. S. Mclntyre, T. E. Rummery, M. G. Cook, and D. Owen, "X-ray photoelectron spectroscopic study of the aqueous oxidation of monel-400," *Journal of Electrochemical Society*, vol. 123, pp. 1164–1170, 1976.

[45] S. Satish Laxman and K. Kar, "Facile synthesis of large area porous Cu_2O as super hydrophobic yellow-red phosphors," *RSC Advances*, vol. 2, no. 9, pp. 3647–3650, 2012.

[46] G. P. Cicileo, B. M. Rosales, F. E. Varela, and J. R. Vilche, "Comparative study of organic inhibitors of copper corrosion," *Corrosion Science*, vol. 41, no. 7, pp. 1359–1375, 1999.

[47] J. F. Bates and J. M. Popplewell, "Corrosion of condenser tube alloys in sulfide contaminated brine," *Corrosion*, vol. 31, no. 8, pp. 269–275, 1975.

[48] H. E. Ostland and J. Alexander, "Oxidation rate of sulfide in sea water, a preliminary study," *Journal of Geophysical Research*, vol. 68, no. 13, pp. 3995–3997, 1963.

[49] P. E. Larson, "X-ray induced photoelectron and auger spectra of Cu, CuO, Cu_2O, and Cu_2S thin films," *Journal of Electron Spectroscopy and Related Phenomena*, vol. 4, no. 3, pp. 213–218, 1974.

[50] D. Chadwick and T. Hashemi, "Benzotriazole adsorption on copper studied by X-ray photoelectron spectroscopy," *Journal of Electron Spectroscopy and Related Phenomena*, vol. 10, no. 1, pp. 79–83, 1977.

[51] D. Chadwick and T. Hashemi, "Adsorbed corrosion inhibitors studied by electron spectroscopy: benzotriazole on copper and copper alloys," *Corrosion Science*, vol. 18, no. 1, pp. 39–51, 1978.

[52] J. F. Moulder, W. F. Stickle, P. E. Sobol, and K. D. Bomben, in *Handbook of X-ray Photoelectron Spectroscopy*, J. Chastain and R. C. King Jr., Eds., Physical Electronics, Inc., Eden Prairie, Minn, USA, 1995.

[53] F. M. Al Kharafi, A. M. Abdullah, I. M. Ghayad, and B. G. Ateya, "Effect of sulfide pollution on the stability of the protective film of benzotriazole on copper," *Applied Surface Science*, vol. 253, no. 22, pp. 8986–8991, 2007.

[54] R. M. Souto, V. Fox, M. M. Laz, M. Pérez, and S. González, "Some experiments regarding the corrosion inhibition of copper by benzotriazole and potassium ethyl xanthate," *Journal of Electroanalytical Chemistry*, vol. 411, no. 1-2, pp. 161–165, 1996.